

# Analytical and Numerical Investigation of the Heat Dissipation in Couette Flow occurring in the Journal Bearing

Kunal Agarwal, Rishabh Aggarwal

(School of Mechanical Engineering, Lovely Professional University, India)

Corresponding Author: Kunal Agarwal

**Abstract:** Heat flux and temperature are the two important parameters that has to be studied in the Plain Journal Bearing. These both the factors affect the working of Plain Journal Bearing very much. Factors like rotational speed of the bearing, the geometry and structure of the bearing, viscosity, irreversibility etc are responsible for the variation in the heat flux and temperature with the change in time.

In our study, change in the heat flux and temperature change is studied for various mineral oils at different rotational speeds of the shaft. The main aim is to select the best mineral oil that could transfer the maximum heat flux out of the system during the working of plain journal bearing at different rotational speed of the shaft and could also produce less irreversibility in the system. While working on the plain journal bearing, some factors such as Reynolds Number, change in kinematic viscosity with the temperature, Viscosity Index, eccentricity etc., are studied and discussed with respect to the present area of research.

**Keywords:** Heat Flux, Temperature, Journal Bearing, Irreversibility, Rotational Speed of the Shaft

Date of Submission: 22-11-2019

Date of Acceptance: 06-12-2019

## Nomenclature

Re	Reynold's Number	$b_z$	Body force in 'z'-direction (N)
$E_G$	Eckert Number	T	Temperature (K)
$P_r$	Prandtl Number	t	Time (sec)
Br	Brinkmann Number	p	Pressure (Pa)
Pe	Peclet Number	$c_p$	Specific heat capacity of the fluid (J/kg-k)
Be	Bejan Number	K	Thermal conductivity of the fluid (w/m-k)
$\rho$	Density of the fluid (kg/l)	H	Vertical gap between the two plates (m)
$\mu$	Dynamic Viscosity of the fluid (Pa-s)	y	Distance along y-axis (m)
$\nu$	Kinematic Viscosity of the fluid (cSt)	VI	Viscosity Index
$\phi$	Viscous Dissipation	$\Omega$	Dimensionless Temperature Difference
$\phi_1$	Irreversibility Distribution Ratio	$u_1$	Tangential Velocity of the shaft (m/s)
$S_G$	Volumetric Rate of Entropy Generation ( $W.m^{-3}.K^{-1}$ )	e	Eccentricity of the shaft (mm)
$N_G$	Entropy Generation Number; Conduction	$\Delta T$	Temperature difference (K)
$N_T$	Entropy Generation Number; Transverse	$q_{max}$	Maximum Heat Flux ( $W/m^2$ )
$N_F$	Entropy Generation Number; Friction	$S_{G(max)}$	Maximum Entropy Generation ( $W.m^{-3}.K^{-1}$ )
$N_S$	Entropy Generation Number; Total	$\bar{q}_{hf1}$	Mean Analytical Heat Flux ( $W/m^2$ )
$q_H$	Heat Flux ( $W/m^2$ )	$\bar{q}_{hf2}$	Mean Quantitative Heat Flux ( $W/m^2$ )
u	Velocity in the 'x'-direction (m/s)	$\bar{e}_1$	Mean Analytical Entropy Generation ( $W.m^{-3}.K^{-1}$ )
v	Velocity in the 'y'-direction (m/s)	$\bar{e}_2$	Mean Quantitative Entropy Generation ( $W.m^{-3}.K^{-1}$ )
w	Velocity in the 'z'-direction (m/s)	r	Correlation
$b_x$	Body force in 'x'-direction (N)		
$b_y$	Body force in 'y'-direction (N)		

## I. Introduction

### 1.1 Bearing

Bearings are used to prevent friction between parts during relative movement. In machinery, they fall into two primary categories: anti-friction or rolling element bearings and hydrodynamic journal bearings. The primary function of a bearing is to carry load between a rotor and the case with as little wear as possible. This bearing function exists in almost every occurrence of daily life from the watch on your wrist to the automobile you drive to the disk drive in your computer. In industry, the use of journal bearings is specialized for rotating machinery both low and high speed.

Heat transfer and temperature rise are the two important factors that affect the working of the plain journal bearing very much. So, the heat transfer and the temperature rise through the bearings has been extensively studied. There were many studies that deals with the heat transfer aspects in the journal bearing especially for non-Newtonian fluids and with rpm of greater than 10,000 rpm but with the heat transfer aspects

in the plain journal bearing with rpm below 10,000 are less. Hence, this study deals with the heat transfer aspects of journal bearings at rotational speed of shaft less than 10,000 rpm. This study particularly relates to the applications of plain journal bearing in hydraulic turbines.

### 1.2 Fluid dynamics

The fluid in the bearing is modelled as given in figure1, with two parallel plates out of which one plate is moving with some constant velocity with respect to the other and the other plate is fixed. The fluid is there between the two plates and it acts as a coolant between the two. This arrangement of the model is studied under the Couette flow analysis [16]. The domain of the study is the area between the two plates.

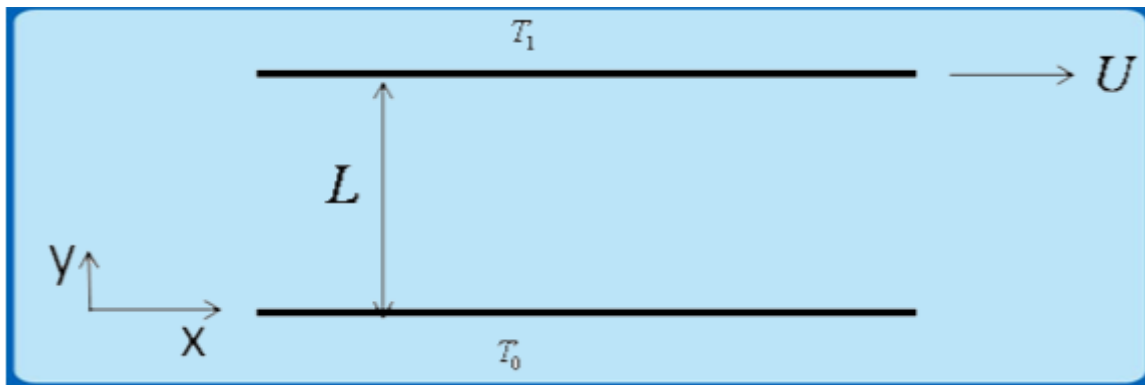


**Figure 1.1 Couette Flow**

### 1.3 Fluid Film Bearing

The primary advantage of a fluid film bearing is often thought of as the lack of contact between rotating parts and thus, infinite life. In a pure sense, this is true, but other complications make this a secondary reason for using these bearings [10]. During the starting of the plain journal bearing, there is momentary metal-to-metal contact and foreign material in the lubricant or excessive vibration can limit the life of a fluid film bearing. For these reasons, special care must be taken when selecting and implementing a lubrication system and special vibration monitoring techniques must be applied. The most important aspects of the health and longevity of a fluid film bearing are proper selection, proper installation, proper lubrication, and the alternating hydrodynamic loads imposed on the bearing surface by relative shaft-to-bearing vibration.

**Some of the primary advantages of fluid film bearings are:**

- Able to withstand shock loads and other abuse.
- Reduce noise.
- Reduce transmitted vibration.
- Provide electrical isolation of rotor to ground.
- Very long life under normal load conditions.
- Wide variety of bearing types for specific application

### 1.4 Importance and Need of the Study

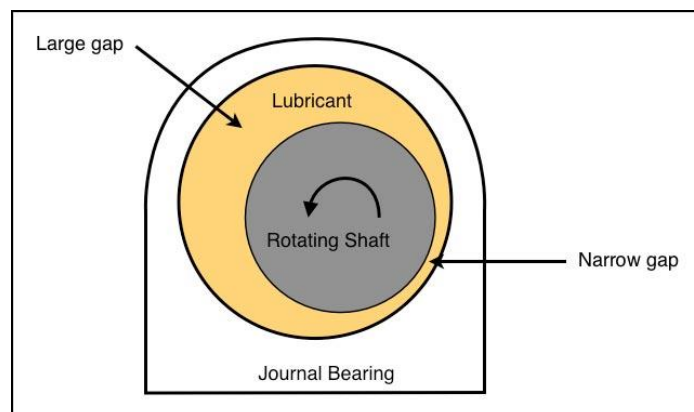


**Figure 1.2 Plain Journal Bearing**

Journal bearings are the most important component to be used in the hydraulic turbines. Especially, the plain journal bearings are the most commonly used bearings in the hydraulic turbines for turbomachinery. Hence, it is important to study the different aspects of the plain journal bearings and especially the heat transfer in the bearing, since these two are the most important parameters that greatly affects the performance of the bearing [5]. To study the plain journal bearing there are some assumptions that needs to be taken and further for the simplification of the study the plain journal bearing can be treated as a classical example of the plain couette flow.

Further, for the study of the bearing the selection of the lubricant is one of the most important factors in the study of the heat transfer for the plain journal bearing. There are various mineral oils that are used at different cases in the bearing but to have a best lubricant that can contain all the important characteristic of a good lubricant for the large range of the rotational speed of the shaft must be find out. Hence, it is important to study the different mineral oils and select the best to be used in the bearing.

### **1.5 Statement of Problem**

The Plain Journal Bearing is a very important component of the hydraulics turbines. In the plain journal bearing, the main point of study will be the heat transfer analysis within the shaft and the housing. The heat transfer analysis is very important in selecting the best possible lubricant for the plain journal bearing that will further have an impact on the cooling effect within the shaft and housing. Therefore, the research problem selected for present study is stated as:

**“Analytical and Numerical Investigation of the Heat Dissipation in Couette Flow occurring in the Journal Bearing”**

### **1.6 Objectives of the Study**

Following are the objectives that were determined for the present study:

- a) To establish the temperature profile for the plain journal bearing.
- b) To study the heat transfer occurring in the plain journal bearing.
- c) To study the entropy generation occurring in the plain journal bearing.
- d) To study the viscosity-temperature relation of various mineral oils.
- e) To select the best possible lubricant for the plain journal bearing.

### **1.7 Assumptions of the Study**

- a) The gap between the two parallel plates is very small. Due to this the viscous dissipation between the two parallel plates becomes very significant.
- b) The flow is completely shear driven that is there is no pressure variation between the flow.
- c) The flow is considered to be laminar.
- d) The flow is considered to be steady.
- e) The flow is considered to be fully developed flow.
- f) The fluid between the two parallel plates is considered to be incompressible.

### **1.8 Hypothesis of the Study**

1. Our model lies in laminar region or not.
2. Analytical Heat Flux values are less than or equal to quantitative heat flux values.
3. Analytical Entropy values are less than or equal to quantitative entropy values.

### **1.9 Tools Used in the Study**

1. **SPSS:** It stands for Statistical Package for Social Science. It is a statistical software package used for Interactive, batched or Statistical analysis. In our study, all the calculation of means, standard deviations and testing of hypothesis are done by using this software. All the graphs between two variables are drawn by using SPSS.
2. **Ansys Workbench:** Ansys workbench is a software to perform structural, thermal and electromagnetic analysis. In our study, it is used to study the temperature change in the plain journal bearing when it rotates at different speeds.
3. **MS Excel:** Excel allows users to perform calculation in a very less time. In our study, all the numerical values of Reynold number, Brinkmann number, heat flux, entropy and Viscosity Index are calculated in Ms Excel by creating the functions of equation.

### 1.10 Variables Used in the Study

Variable is defined as anything that has the quantity and quality that varies. In our study, Variables are classified as:

**Dependent Variables:** A dependent variable is the variable being tested and measured in the study. In our study, dependent variables are viscosity, heat flux, brinkmannnumber and entropy etc

**Independent Variable:** An independent variable is the variable that is changed in the study to test its effect on dependent variable. In our study the independent variables are temperature and rotational speed of the shaft.

### 1.11 Technical Terms used in the Study

1. **Viscosity:** Viscosity is a measure of the resistance of a fluid to deformation under shear stress. Viscosity describes a fluid's internal resistance to flow and may be thought of as a measure of fluid friction.
2. **Viscosity index:** Viscosity index is a dimensionless number that represents how the viscosity of a hydraulic fluid changes with temperature. A fluid with a low viscosity index will experience a relatively large swing in viscosity as temperatures change.
3. **Laminar Flow:** In laminar flows, fluid layers slide in parallel, with no eddies, swirls or currents normal to the flow itself. This type of flow is also referred to as streamline flow. Here, the viscous forces are higher than the inertial forces.
4. **Reynolds Number** is a macroscopic parameter of a flow in its globality and defines the region of the fluid that it will be either laminar or transient or turbulent.
5. **Steady State Flow:** This refers to a condition where the fluid properties at any single point in the system do not change with time. These properties are temperature, velocity and pressure. Also, the system mass flow rate is constant.
6. **Heat Flux:** Heat flux is the thermal energy transferred from one substance to another per unit time and area denoted by temperature change measured in watts per meter squared units. The heat flow rate is defined as the amount of heat transferred per unit time in the material.
7. **Prandtl No.:** The Prandtl number is a dimensionless number, defined as the ratio of momentum diffusivity to thermal diffusivity. Prandtl number is not dependent on geometry of an object involved in the problem but is dependent solely on the fluid and the fluid state.
8. **Eckert number:** The Eckert number is a dimensionless number, is defined as the ratio of the advective mass transfer to the heat dissipation potential. The Eckert number provides a measure of the kinetic energy of the flow relative to the enthalpy difference across the thermal boundary layer. It is used to characterize heat dissipation in high-speed flows for which viscous dissipation is significant.
9. **Brinkmann Number:** It is the ratio between heat produced by viscous dissipation and heat transported by molecular conduction. i.e., the ratio of viscous heat generation to external heating. The higher its value, the slower the conduction of heat produced by viscous dissipation and hence the larger the temperature rise.
10. **Entropy:** Entropy is defined as the number of ways a system can be arranged. The higher the entropy, the more the system is disordered. According to the second law of thermodynamics, in any process that involves a cycle, the entropy of the system will either stay the same or increase
11. **Viscous Dissipation:** It is a phenomenon of conversion of mechanical energy into thermal. It accounts for the loss in the form of heat.

## II. Literature Review

### 2.1 Reynolds Number

The Reynolds Number plays a prominent role in foreseeing the patterns in a fluid's behaviour. It is a dimensionless number and denoted as  $Re$ . It is used to determine whether the fluid flow is laminar or turbulent. Laminar flow occurs when a fluid flows in parallel layers with no disruption between the layers. In laminar fluid

flow, the fluid flows at a constant speed. Turbulent flow occurs when the fluid undergoes irregular fluctuations. In turbulent flow, the flow of the fluid is continuously undergoing changes in both magnitude and direction.

In practice, matching the Reynolds Number is not on its own sufficient to guarantee similitude. Fluid flow is generally chaotic and very small changes to shape and surface roughness can result in very different flows. Nevertheless, Reynolds Number are a very important guide and are widely used during the study of fluid flows.

Reynold number is one of the main controlling parameters in all viscous flows where a numerical model is selected according to pre-calculated Reynold Number. Reynold Number is the ratio of the Inertial Forces and Viscous Forces. It is calculated as:

$$Re = \frac{\rho v d}{\mu}$$

Ranges of the Reynold number to select the region are:

For Laminar Flow,	Re < 2100
For Transient Flow,	2100 < Re < 4000
For Turbulent Flow,	Re > 4000

## 2.2 Eccentricity in Plain Journal Bearing

Eccentricity is equal to the difference between the radius of the bearing and the radius of the journal (the radial oil clearance). A great difference between their radii (or diameters) helps to establish stable hydrodynamic lubrication, especially at high rotation speed.

If the eccentricity is too high there is a risk of metal to-metal contact and higher dynamic loads being imparted to the babbitt causing premature fatigue [10]. If the eccentricity is too low (journal is nearly centered) then the machine could more easily become unstable. Eccentricity is a function of both speed and load.

A graph is plotted in Figure 2.1 that shows the variation of the eccentricity ratio with the rotational speed of the plain journal bearing at a constant load. On the basis of this graph, eccentricity at different rotational speed is observed and is used designing the plain journal bearing in the Ansys Workbench.

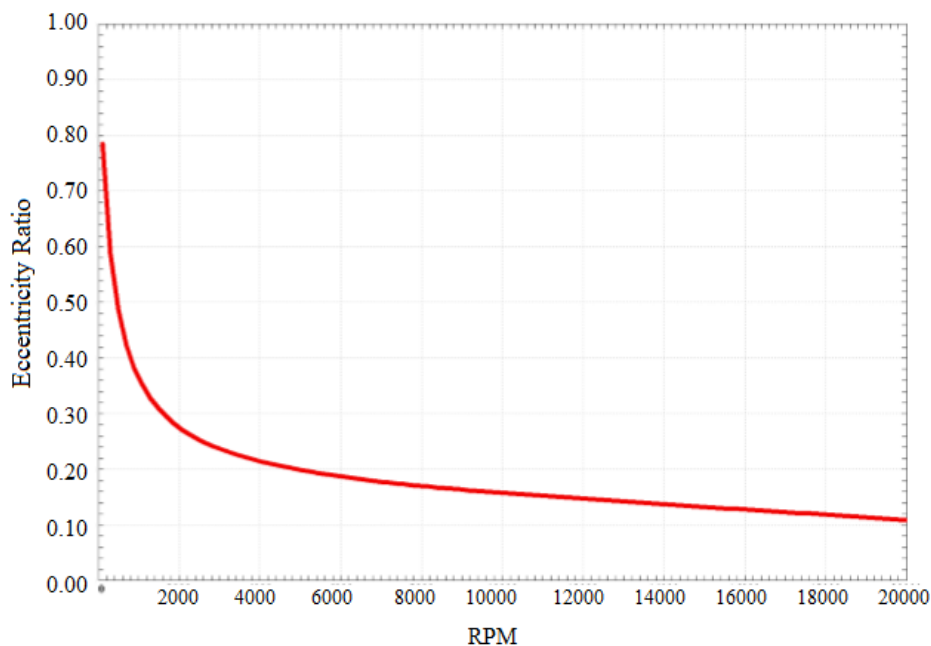


Figure 2.1 Plain Bearing Eccentricity Versus Speed with a Constant Load [10]

## 2.3 Viscosity as a function of temperature with RPM

As the hydrodynamic behaviour of plain journal bearings is totally dependent on the viscosity characteristics of the lubricant. The viscosity grade required is dependent upon bearing speed, oil temperature and load. Table 2.1 provides a general guideline to selecting the correct ISO viscosity grade [15]. The ISO grade number indicated is the preferred grade for the speed and temperature range. ISO 68- and 100- Grade oils are commonly used in indoor, heated applications, with ISO32- grade oils being used for high-speed (10,000 rpm) units and some outdoor low temperature applications. The higher the bearing speed, the lower the oil viscosity

required and also that the higher the unit operating temperature, the higher the oil viscosity required. If vibration or minor shock loading is possible, a higher grade of oil than the one indicated in the below table 2.1 should be considered.

**Table 2.1 Plain Bearing ISO Viscosity Grade Selection**

Bearing Speed (rpm)	Bearing / Oil temperature (Degree Celsius)		
	60 <sup>o</sup> C	75 <sup>o</sup> C	90 <sup>o</sup> C
300 – 1,500	-	ISO 68	ISO 100 – 150
1,800	ISO 32	ISO 32 – 46	ISO 68 – 100
3,600	ISO 32	ISO 32	ISO 46 - 68
10,000	ISO 32	ISO 32	ISO 32

**2.4 Importance of Viscosity Index**

Viscosity is a physical measurement of a fluid’s internal resistance to flow. Assume that a lubricating fluid is compressed between two flat plates, creating a film between the plates. Force is required to make the plates move, or overcome the fluid’s film friction. This force is known as dynamic viscosity. Dynamic viscosity is a measurement of a lubricant’s internal friction and it is usually reported in units called poise (P) or centipoise (1 P = 0.01 cP). Every mineral oil has its own viscosity and it always changes with the change in temperature in the system. So, it is very important to study the effect of temperature on the viscosity. To do so, a parameter named Viscosity Index is calculated.

Viscosity index [2] is the change in the viscosity between two different temperatures. Generally, we take two temperatures at 40 and 100 Degree Celsius. Higher the viscosity index means lower the change in viscosity of the oil with temperature.

Generally, lubricant oil of less viscosity is taken to form a film layer in the plain journal bearing. But viscosity should not be very less so that the existence of the lubrication film layer will be neglected and friction b/w two sliding surfaces will take place. To overcome this problem, oil of appropriate lesser viscosity is taken. So, our consideration is select a mineral oil of less viscosity up to a certain lesser limit.

When the journal bearing starts to rotate, the temperature tends to increase inside the plain journal bearing either may be due to viscous heating or any other reason and it reaches up to a maximum value of 90°C. It is observed that viscosity always decreases with the increase in the temperature. Now to fulfil the requirement of selecting mineral oil with less variation in the viscosity with the increase in temperature, Viscosity Index is calculated.

$$\text{Viscosity Index Value} \propto \frac{1}{\text{Viscosity change with temperature}}$$

Higher value of Viscosity Index signifies the less change in the viscosity of the mineral oil with the increase in the temperature.

**2.5 Heat Generation and Temperature Rise in the Plain Journal Bearing**

The most important factor to be considered while analysing the plain journal bearings or in general case the journal bearings are the heat generation within the lubricant film and the corresponding temperature rise that takes place within the lubricant film [8]. These two factors are the most important factors while selecting the best possible lubricant for the plain journal bearings. Generally, the temperature rise in the lubricant film must be small that will signify the stable or good conditions of the journal bearing. The problems of heat generation and the temperature rise are hard to handle practically but with the help of various analytical tools like ANSYS they can be handled properly and hence the problem of any case of model can be handled.

The heat generation in the journal bearing takes place due to the shear in the lubricant film that corresponds to the loss of the mechanical energy within the lubricant film and hence the heat is generated in the system. Generally, this heat generated is called as viscous heating. This is basically a loss in the system and is needed to be decreased. The lesser the heat generated the better is the operating condition of the plain journal bearing.

The problem of the temperature rise is more important than the heat generation since due to the temperature rise the viscosity of the lubricating film decreases and thus the minimum oil thickness and therefore allowing the seizure to occur more easily. The temperature rise also changes the bearing clearance that occurs through the thermal deformation of the bearing metal and thus the performance of the plain journal bearing gets affected and the bearing performance decreases.

The temperature rise also causes a much bigger problem by decreasing the boundary lubrication performance and it will be completely lost if the lubricant temperature exceeds a certain critical temperature. The lubricating film will have a transition temperature and major changes will occur if the temperature of the lubricant will go less or above the transition temperature. If the lubricant temperature is less than the transition temperature then the molecules of the lubricant will combine with the metal surface strongly and also with the adjacent molecules of the lubricant and will form a strong lubrication film on the metal surface. But if the temperature of the lubricant film will go above the transition temperature then the strength of the lubrication film will decrease remarkably which will also pose greater problem for the system and the seizure can take place very easily. Thus, the lubrication temperature must be less than the transition temperature. The transition temperature is unfortunately very low for the oils.

1. For low cost oils the transition temperature is 100°C
2. For high cost oils the transition temperature is 160°C-170°C

Now if the oil temperature goes beyond 150°C then the degradation of the oil will be there and the rate of oxidation will be increased remarkably. At 100°C the tensile strength of the metal falls to one half to that at room temperature. Thus, it is required to keep the highest temperature in the bearing lower than 100°C-120°C.

Thus, it is very important to know the highest temperature in the bearing with the particular type of the lubricant used in the bearing.

## **2.6 Measurement of Temperature in Fluid Film Bearing**

Temperature is the only parameter in the journal bearing that can be used to monitor the performance of the bearing. The temperature of the drain oil spilling from the bearing can be easily recorded and traditionally it has been used to monitor the performance of the bearing but unfortunately the oil temperature is not a good parameter to monitor since it has poor sensitivity and response to changing conditions within the bearing. The classic example of this is the case of the bearing lining breakup in the plain journal bearing. Hence, it is far better to record the temperature of the bearing in the active regions where higher sensitivity and response exists. This is pretty much important so that the failure temperature can be given according to the bearing lining material [7]. Most bearings are designed to operate well below the failure temperature. The alarm can be put to safeguard against relatively gradual but potentially dangerous changes in the bearing.

The temperature sensors are used to record the temperature in the oil film. The temperature sensors used are:

- Thermocouple
- Resistance Temperature Detector (RTD)

## **2.7 Entropy Generation**

The phenomenon of entropy generation can be seen with all types of heat transfer problems and it is generally associated with the thermodynamic irreversibility. There are many sources of the entropy generation in the system like heat transfer across the finite temperature gradient, characteristic of convective heat transfer, viscous effect etc. The generation of entropy actually destroys the available work of the system [17]. Thus, it is very important to study the irreversibility in the heat transfer problems and especially where the fluid flow processes are involved.

In the plain journal bearing the study of entropy generation is used to investigate the effects of irreversibility which can be clearly seen through the temperature rise. The entropy generation in the plain journal bearings plays a major role in deciding the best possible lubrication for the bearing. The entropy generation must be low so that the maximum available work can be there with the system and there is less work lost. Thus, the entropy generation analysis must be done for the present study.

Following the basis of our model the entropy equation is stated in the section(3.4). According to the equation stated the first term of that equation represents the entropy generation due to the heat transfer and the second term represents the entropy generation due to the viscous dissipation. Further in the non-dimensional form, the entropy generation can be broken into three components ( $N_C, N_Y, N_F$ ) which further represents the causes for the entropy generation. ' $N_C$ ' represents the entropy generation by heat transfer due to axial conduction. This occurs when there is a temperature difference in the x-direction, but in our model, there is no temperature difference in the x-direction. Hence, the value of ' $N_C$ ' becomes zero. ' $N_Y$ ' represents the entropy generation due to heat transfer in the normal direction to the axis. This component of entropy generation is not zero in our study since in our model there is a variation in the y-direction. ' $N_F$ ' represents the entropy generation due to the fluid friction.

## **2.8 Fluid Friction versus Heat Transfer Irreversibility**

The presence of Irreversibility in the system is the main cause for the entropy generation. This presence of Irreversibility is there in almost every problem of heat transfer. Both the fluid friction and the heat transfer contribute to the rate of the entropy generation. The expression for entropy generation stated in the section (3.4)

is good for generating the spatial profile for the entropy but not able to tell that whether the fluid friction dominates or the heat transfer [18]. This problem is solved by the Irreversibility Distribution Ratio( $\phi_1$ ) which is defined as the ratio of the entropy generation due to the fluid friction ( $N_F$ ) to the entropy generation due to the heat transfer ( $N_C + N_Y$ ). With this the three conditions arises about the Irreversibility Distribution Ratio:

1. When ( $0 \leq \phi_1 < 1$ ), the heat transfer dominates for generating the entropy
2. When ( $\phi_1 > 1$ ), the fluid friction dominates for generating the entropy
3. When ( $\phi_1 = 1$ ), the heat transfer and the fluid friction have same contribution for generating the entropy

Mathematically,

$$\phi_1 = \frac{N_F}{N_C + N_Y}$$

But in many cases apart from the heat transfer and the fluid friction dominance the contribution of the heat transfer ( $N_C + N_Y$ ) on the overall entropy generation rate ( $N_S$ ) is needed. Thus, for this purpose as an alternative to Irreversibility Distribution Ratio( $\phi_1$ ), Bejan Number is used which is defined as the ratio of the entropy generation due to the heat transfer to the total entropy generation. Here again three cases arise:

1. When ( $Be = 1$ ), the heat transfer irreversibility dominates.
2. When ( $Be = 0$ ), the fluid friction irreversibility dominates.
3. When ( $Be = 0.5$ ), the heat transfer and the fluid friction entropy generation rates are equal.

Mathematically,

$$Be = \frac{N_C + N_Y}{N_S} = \frac{1}{1 + \phi_1}$$

### III. Research Methodology

#### 3.1 Navier-Stokes Equation:

The Navier-Stokes equations govern the motion of the fluids and can be seen as Newton's second law of motion for fluids. The Navier-Stokes equations represent the conservation of momentum and can be used to formulate the velocity profiles for the research model.

In 'x'-direction [4]:

$$\frac{\partial u}{\partial t} + u \frac{\partial u}{\partial x} + v \frac{\partial u}{\partial y} + w \frac{\partial u}{\partial z} = -\frac{1}{\rho} \frac{\partial p}{\partial x} + \nu \left[ \frac{\partial^2 u}{\partial x^2} + \frac{\partial^2 u}{\partial y^2} + \frac{\partial^2 u}{\partial z^2} \right] + \nu \frac{\partial}{\partial x} \left( \frac{1}{3} * \nabla \cdot v \right) + b_x$$

... (1)

Now solving the above equation as per the assumed model of the Couette Flow we have:

For hydrodynamically fully developed flow

$$\frac{\partial u}{\partial x} = 0$$

So therefore, we have

$$\frac{\partial^2 u}{\partial x^2} = 0$$

Since there is no pressure variation along the x-direction we have

$$\frac{\partial p}{\partial x} = 0$$

Since the model problem is considered to be 2 dimensional or the dimensions in the z direction is very large and any variation with respect to z can be neglected, we have

$$\frac{\partial u}{\partial z} = 0$$

So therefore

$$\frac{\partial^2 u}{\partial z^2} = 0$$

Since the effect of gravity is neglected, we have,

$$b_x = 0$$

Since the flow is considered to be steady, we have,

$$\frac{\partial u}{\partial t} = 0$$

Since the flow is considered to be incompressible, we have,

$$\nabla \cdot v = 0$$

Hence, the equation (1) is reduced to

$$\frac{\partial^2 u}{\partial y^2} = 0 \quad \dots (2)$$

Now solving the equation (2)

$$\frac{du}{dy} = c_1$$

$$u = c_1y + c_2 \quad \dots (3)$$

Applying the Boundary conditions

1 - At  $y = 0, u=0$  Since there is no slip condition at the lower plate

2 - At  $y = H, u=u_1$  Since the upper plate is given the velocity of  $u_1$

Now solving the equation (3) using the boundary conditions we get

$$u = u_1 * \frac{y}{H} \quad \dots (4)$$

**In 'y'-direction [4]:**

$$\frac{\partial v}{\partial t} + u \frac{\partial v}{\partial x} + v \frac{\partial v}{\partial y} + w \frac{\partial v}{\partial z} = -\frac{1}{\rho} \frac{\partial p}{\partial y} + \nu \left[ \frac{\partial^2 v}{\partial x^2} + \frac{\partial^2 v}{\partial y^2} + \frac{\partial^2 v}{\partial z^2} \right] + \nu \frac{\partial}{\partial y} \left( \frac{1}{3} * \nabla \cdot v \right) + b_y \quad \dots(5)$$

Now solving the above equation as per the assumed model of the Couette Flow we have:

Since the flow is considered to be steady, we have,

$$\frac{\partial v}{\partial t} = 0$$

Since the flow is considered to be incompressible, we have,

$$\nabla \cdot v = 0$$

Since the effect of gravity is neglected, we have,

$$b_y = 0$$

Since the model problem is considered to be 2 dimensional or the dimensions in the 'z' direction is very large and any variation with respect to 'z' can be neglected we have,

$$\frac{\partial v}{\partial z} = 0$$

So therefore,

$$\frac{\partial^2 v}{\partial z^2} = 0$$

Now applying the continuity equation for the incompressible fluid flow, we have,

$$\frac{\partial u}{\partial x} + \frac{\partial v}{\partial y} + \frac{\partial w}{\partial z} = 0 \quad \dots(6)$$

For hydrodynamically fully developed flow we have,

$$\frac{\partial u}{\partial x} = 0$$

Since the model problem is considered to be 2 dimensional or the dimensions in the 'z' direction is very large and any variation with respect to 'z' can be neglected we have,

$$\frac{\partial w}{\partial z} = 0$$

Hence from the continuity equation (6) we get,

$$\frac{\partial v}{\partial y} = 0$$

Therefore,

$$\frac{\partial^2 v}{\partial y^2} = 0$$

Since the plates are considered to be made of non-porous materials hence the value of  $v = 0$

Therefore,

$$\frac{\partial v}{\partial x} = 0$$

Hence the equation (5) gets reduced to,

$$-\frac{1}{\rho} * \frac{\partial p}{\partial y} = 0 \quad \dots(7)$$

Solving the equation (7) we get,

$$\frac{\partial p}{\partial y} = 0$$

Therefore,

$$p = \text{constant}$$

Hence, there is no pressure variation in the 'y' direction.

**In 'z'-direction [4]:**

$$\frac{\partial w}{\partial t} + u \frac{\partial w}{\partial x} + v \frac{\partial w}{\partial y} + w \frac{\partial w}{\partial z} = -\frac{1}{\rho} \frac{\partial p}{\partial z} + \nu \left[ \frac{\partial^2 w}{\partial x^2} + \frac{\partial^2 w}{\partial y^2} + \frac{\partial^2 w}{\partial z^2} \right] + \nu \frac{\partial}{\partial z} \left( \frac{1}{3} * \nabla \cdot v \right) + b_z \quad \dots(8)$$

In the above equation all the values of the individual expressions correspond to zero since the problem is considered to be 2 dimensional and any variation with respect to the 'z' direction can be neglected. Hence, by solving the Navier Stokes equation we get the velocity profile in the Couette flow.

### 3.2 Heat Flux Equation:

Let us assume that the temperature between the two plates is a function of 'y' direction only. Now since the plates are at isothermal temperature and the duct is very large so the temperature seems to be a function of 'x' direction [4].

#### Writing the thermal energy equation:

$$\rho c_p \left[ \frac{\partial T}{\partial t} + u \frac{\partial T}{\partial x} + v \frac{\partial T}{\partial y} + w \frac{\partial T}{\partial z} \right] = K \left[ \frac{\partial^2 T}{\partial x^2} + \frac{\partial^2 T}{\partial y^2} + \frac{\partial^2 T}{\partial z^2} \right] + \mu * \phi \dots(9)$$

Now solving the equation (9) as per the assumed model of the Couette Flow we have:

Since, the problem is considered to be steady, we have,

$$\frac{\partial T}{\partial t} = 0$$

Since, the temperature is not a function of 'x' we have,

$$\frac{\partial T}{\partial x} = 0$$

Hence,

$$\frac{\partial^2 T}{\partial x^2} = 0$$

Since, the plates are non-porous we have,

$$v = 0$$

Since, the problem is considered to be 2-dimensional, we have,

$$\frac{\partial T}{\partial z} = 0$$

Hence,

$$\frac{\partial^2 T}{\partial z^2} = 0$$

Hence the above thermal energy equation reduces to

$$K \left[ \frac{\partial^2 T}{\partial y^2} \right] + \mu * \phi = 0 \quad \dots(10)$$

Here  $\phi$  is given by:

$$\phi = \frac{2}{3} \left[ \left( \frac{\partial u}{\partial x} - \frac{\partial v}{\partial y} \right)^2 + \left( \frac{\partial u}{\partial x} - \frac{\partial w}{\partial z} \right)^2 + \left( \frac{\partial v}{\partial y} - \frac{\partial w}{\partial z} \right)^2 \right] + \left[ \left( \frac{\partial u}{\partial y} + \frac{\partial v}{\partial x} \right)^2 + \left( \frac{\partial u}{\partial z} + \frac{\partial w}{\partial x} \right)^2 + \left( \frac{\partial v}{\partial z} + \frac{\partial w}{\partial y} \right)^2 \right] \quad \dots(11)$$

From the Navier Stokes equation we have proved that the velocity 'u' is a function of only y direction and not of any other direction.

Hence, the equation (11) reduces to

$$\phi = \left( \frac{\partial u}{\partial y} \right)^2 \quad \dots(12)$$

From the results of the Navier Stokes equation we have,

$$u = u_1 * \frac{y}{H}$$

Putting the value of the velocity in the equation (12) we get

$$\phi = \frac{u_1^2}{H^2} \quad \dots(13)$$

Putting the value of the viscous dissipation obtained in equation (13) in the equation (10) we get,

$$K * \frac{d^2 T}{dy^2} + \mu * \frac{u_1^2}{H^2} = 0 \quad \dots(14)$$

Solving the equation (14) we get,

$$\frac{dT}{dy} + \frac{\mu u_1^2}{K H^2} * y = c_3$$

$$T + \frac{\mu u_1^2}{K H^2} * \frac{y^2}{2} = c_3 * y + c_4 \quad \dots(15)$$

Applying the Boundary conditions to solve the equation (15):

At  $y=0, T=T_0$

Putting the above condition in the equation (15) we get,

$$c_4 = T_0$$

At  $y=H, T=T_1$

Applying the above condition in equation (15) we get,

$$T_1 + \frac{\mu u_1^2}{K H^2} * \frac{H^2}{2} = c_3 * H + T_0$$

Therefore, the value of 'c<sub>3</sub>' comes out to be

$$c_3 = \frac{T_1 - T_0}{H} + \frac{\mu u_1^2}{2KH}$$

Hence the temperature profile becomes,

$$T - T_0 = (T_1 - T_0) \frac{y}{H} + \frac{\mu u_1^2}{2K} \left( \frac{y}{H} - \frac{y^2}{H^2} \right)$$

... (16)

### 3.2.1 Heat Flux at the Top Plate:

Applying the thermal conduction equation at the interface of the fluid film and the plate we have [4],

$$q_H = -K \frac{dT}{dy} \quad \dots(17)$$

From equation (16),

$$\frac{dT}{dy} = \frac{T_1 - T_0}{H} + \frac{\mu u_1^2}{2k} \left[ \frac{1}{H} - \frac{2y}{H^2} \right]$$

At  $y=H$ ,

$$\frac{dT}{dy} = \frac{T_1 - T_0}{H} - \frac{\mu u_1^2}{2kH} \quad \dots (18)$$

Putting equation (18) in the equation (17), we get

$$q_H = \frac{-K(T_1 - T_0)}{H} \left[ 1 - \frac{u_1^2 \mu c_p}{2 c_p (T_1 - T_0) k} \right]$$

$$q_H = \frac{-K(T_1 - T_0)}{H} \left[ 1 - \frac{Ec \cdot Pr}{2} \right] \quad \dots(19)$$

### 3.2.2 Heat Flux at the Bottom Plate:

Applying the thermal conduction equation at the interface of the fluid film and the plate we have [4],

$$q_H = -K \frac{dT}{dy}$$

From equation (16),

$$\frac{dT}{dy} = \frac{T_1 - T_0}{H} + \frac{\mu u_1^2}{2k} \left[ \frac{1}{H} - \frac{2y}{H^2} \right]$$

At  $y=0$ ,

$$\frac{dT}{dy} = \frac{T_1 - T_0}{H} + \frac{\mu u_1^2}{2kH} \quad \dots (20)$$

Putting equation (18) in the equation (17), we get

$$q_H = \frac{-K(T_1 - T_0)}{H} \left[ 1 + \frac{u_1^2 \mu c_p}{2 c_p (T_1 - T_0) k} \right]$$

$$q_H = \frac{-K(T_1 - T_0)}{H} \left[ 1 + \frac{Ec \cdot Pr}{2} \right] \quad \dots(21)$$

Here,

$$Ec = \frac{u_1^2}{c_p (T_1 - T_0)}$$

$$Pr = \frac{\mu c_p}{K}$$

$$Br = Ec * Pr = \frac{u_1^2 \mu}{(T_1 - T_0) k} \quad \dots(22)$$

### 3.3 Second Law Analysis

On the basis of second law of thermodynamics and assumptions already made [17], the local volumetric rate of entropy generation i.e.  $S_G(\text{W.m}^{-3} \cdot \text{K}^{-1})$

$$S_G = \frac{k}{T_0^2} \left[ \left( \frac{\partial T}{\partial x} \right)^2 + \left( \frac{\partial T}{\partial y} \right)^2 \right] + \frac{\mu}{T_0} \left[ \left( \frac{\partial u}{\partial x} \right)^2 \right] \dots (23)$$

Applying the same parameters used for scaling earlier the dimensionless form of above equation is:

$$N_S = S_G \frac{kT_0^2}{q^2} = \frac{1}{Pe^2} \left[ \left( \frac{\partial T}{\partial X} \right)^2 \right] + \left[ \left( \frac{\partial T}{\partial Y} \right)^2 \right] + \frac{Br}{\Omega} \left[ \left( \frac{\partial U}{\partial Y} \right)^2 \right]$$

$$N_S = N_C + N_Y + N_F$$

### 3.4 Temperature-Viscosity Equation

Mainly two equations define the relationship of viscosity and temperature. But equation is chosen based on the type of viscosity i.e. kinematic viscosity or dynamic viscosity [6].

**Table 3.1 Viscosity-Temperature Equations**

Name	Equation	Comment
Reynolds [6]	$\mu_0 = be^{-aT_A}$	Early equation, accurate only for a limited temperature range
Slotte [6]	$\mu_0 = \frac{a}{(b + T_A)^c}$	Reasonable, useful for numerical analysis
Vogel [6]	$\mu_0 = ae^{\frac{b}{(T-c)}}$	If we are having dynamic viscosities
Walter [6]	$\log \log(z) = a - b \log T$	If we are having kinematic viscosities

Where,

$\mu_0$  = dynamic viscosity

$\nu_0$  = kinematic viscosity

T = absolute temperature in Kelvin

a, b, c are the constants

In our study, for calculation of numerical values of kinematic viscosity, at specific temperature, Walter equation is used. This Walter equation is given by ASTM in its test method D341 – 03 [3]. This equation is valid for the range of kinematic viscosity i.e.  $2 * 10^7$  to  $0.21 \text{ cSt}$

$$\log \log(z) = a - b \log T \dots (24)$$

Where,

$Z = (\nu + 0.7)$  if  $\nu = 2 * 10^7$  to  $2.00 \text{ cSt}$

$Z = (\nu + 0.7 + C)$  if  $\nu = 2 * 10^7$  to  $1.65 \text{ cSt}$

$Z = (\nu + 0.7 + C - D)$  if  $\nu = 2 * 10^7$  to  $0.90 \text{ cSt}$

$Z = (\nu + 0.7 + C - D + E)$  if  $\nu = 2 * 10^7$  to  $0.30 \text{ cSt}$

$Z = (\nu + 0.7 + C - D + E - F + G)$  if  $\nu = 2 * 10^7$  to  $0.24 \text{ cSt}$

$Z = (\nu + 0.7 + C - D + E - F + G - H)$  if  $\nu = 2 * 10^7$  to  $0.21 \text{ cSt}$

In which,

$C = \exp(-1.14883 - 2.65868 \nu)$ ,

$D = \exp(-0.0038138 - 12.5645 \nu)$ ,

$E = \exp(5.46491 - 37.6289 \nu)$ ,

$F = \exp(13.0458 - 74.6851 \nu)$ ,

$G = \exp(37.4619 - 192.643 \nu)$ , and

$H = \exp(80.4945 - 400.468 \nu)$ .

### 3.5 Viscosity Index Equation

To calculate Viscosity Index, ASTM D2270 [2] method is used. Viscosity Index is calculated always at 40 and 100 degrees celsius for a particular ISO grade of lubricant.

Calculate the viscosity index, VI, of the oil as follows:

$$VI = \left[ \frac{((\text{antilog} N) - 1)}{0.00715} \right] + 100 \dots (25)$$

$$N = \frac{\log H - \log U}{\log Y}$$

where:

Y = kinematic viscosity at 100°C of the oil whose kinematic viscosity is to be calculated,  $mm^2/s$  (cSt), and  
 H = kinematic viscosity at 40°C of an oil of 100 Viscosity Index having the same kinematic viscosity at 100°C as the oil whose viscosity index is to be calculated  $mm^2/s$  (cSt).

U = kinematic viscosity at 40°C of the oil whose viscosity index is to be calculated  $mm^2/s$  (cSt).

**There are two cases to calculate H value:**

**Case1:** If the kinematic viscosity of the oil at 100°C is in the range of 2 to 70  $mm^2/s$  (cSt), extract the corresponding value for H from the ASTM D2270-04 method. Measured values that are not listed, but are within the range of table mentioned in ASTM D2270-04 method, can be obtained by linear interpolation. The viscosity index is not defined and may not be reported for oils of kinematic viscosity of less than 2.0  $mm^2/s$  (cSt) at 100°C.

**Case2:** If the measured kinematic viscosity at 100°C is greater than 70  $mm^2/s$  (cSt), calculate the value of H as follows:

$$H = 0.1684 Y^2 + 11.85 Y - 97$$

**3.6 Statistical Methods**

Statistic and its different methods are the key base research process. They provide an indispensable tool for collecting, organizing, analysing and interpreting data expressed in numerical terms. By synthesizing the data, these methods can facilitate the derivation of conclusion and formulation of generalizations.

**3.6.1 Mean**

The mean [18] of a distribution is commonly understood as the arithmetic average.

$$\mu = \frac{\sum x}{n}$$

Where,

$$\begin{aligned} \mu &= \text{Mean} \\ \sum x &= \text{Sum of Data Points} \\ n &= \text{No of Data Points} \end{aligned}$$

**3.6.2 Standard Deviation**

Standard deviation [18] tells about the deviation or variation of our calculated results from the actual results or mean value.

$$\sigma = \sqrt{\frac{(x - \bar{x})^2}{n - 1}}$$

Where,

$\sigma$  = Standard Deviation

$x$  = Data value

$\bar{x}$  = Mean value

$n$  = no of data points

**3.6.3 Hypothesis Testing**

It will be done to compare our manually calculated results with the analytical results within the range of 5% error. Hypothesis testing will help in concluding the final results of our study.

**3.6.4 Correlation**

Correlation [18] is the study of the dependency of one variable on another variable. It tells that by how much percent one variable will change due to the change of another variable. To do so, correlation value and coefficient of determination is found out.

$$r = \frac{\sum(x - \bar{x})(y - \bar{y})}{\sqrt{\sum(x - \bar{x})^2 \sum(y - \bar{y})^2}}$$

Where,

$r$  = Correlation value

$x$  = independent variable i.e. Heat Flux

$y$  = dependent variable i.e. RPM

$r^2$  = coefficient of determination

#### IV. Geometrical Configuration for Numerical and Analytical Simulation

Technical Data used for the Numerical Simulation	
Shaft Radius	$R_S = 0.05m$
Journal Radius	$R_B = 0.1m$
Radial Clearance	$C = 0.05m$
Reference Temperature	$T_0 = 303 K$
Reference Pressure	$P = 1 atm$
Initial Temperature of the lubrication	$T_L = 303 K$
Lubrication Density	$\rho = 827.1 kg/m^3$
Lubrication Specific Heat	$C_p = 1942.67 J/Kg-K$
Lubrication Thermal Conductivity	$K = 0.128 W/m-k$
Lubrication Viscosity	$\mu = 0.013 Pa-s$
Bearing Thermal Conductivity	$k_b = 54 W/m-k$
Bearing Density	$\rho = 7833 kg/m^3$
Bearing Specific Heat	$C_p = 465 J/Kg-K$
Bearing Convective Heat Transfer Coefficient	$h_B = 80 W/m^2 - k$
Shaft Convective Heat Transfer Coefficient	$h_S = 100 W/m^2 - k$
Revolution Speed	$N = 1000 \text{ to } 2000 \text{ rpm}$

The above technical data is used to model the journal bearing in the Ansys Workbench.

#### 4.1 Modelling of Journal Bearing

As discussed in section 2.2, considering the effect of eccentricity to model the journal bearing in Ansys, is very important. From the figure 2.1, eccentricity values are observed at different rotational speeds of the shaft and are tabulated in table 4.1:

**Table 4.1 Eccentricity at Various RPM for Plain Journal Bearing [10]**

RPM	e/H	e (mm)
1000	0.35	17.5
1250	0.32	16
1500	0.3	15
1750	0.29	14.5
2000	0.27	13.5

#### 4.2 Meshing Results of the Model

In the Ansys Software the design of the model is made according to the various rotational speeds of the shaft and eccentricity values respectively. In the meshing domain, under sizing the ‘relevance center’ was kept as medium and ‘smoothing’ was kept as high. The faces were mapped in the shape of the quadrilaterals and the refinement was kept at 2. The meshing results obtained through numerical simulation are shown from the figure 4.1 to figure 4.5:

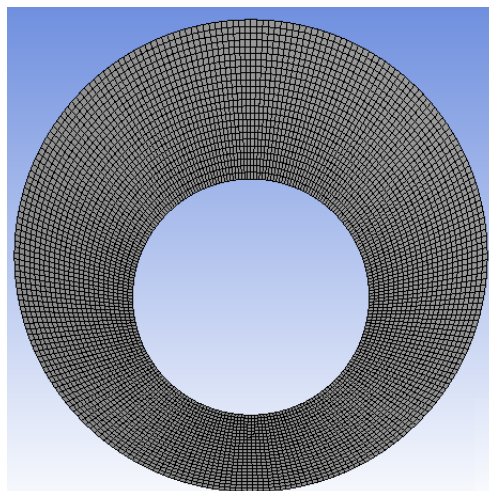


**Figure 4.1 Mesh result for the model at N=1000**  
Meshing Quality - 0.958

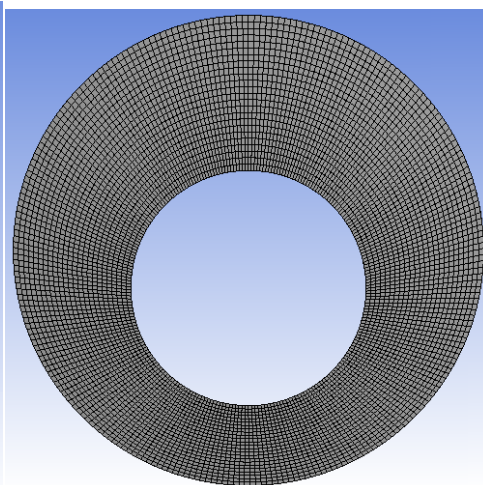


**Figure 4.2 Mesh result for the model at N=1250**  
Meshing Quality - 0.964

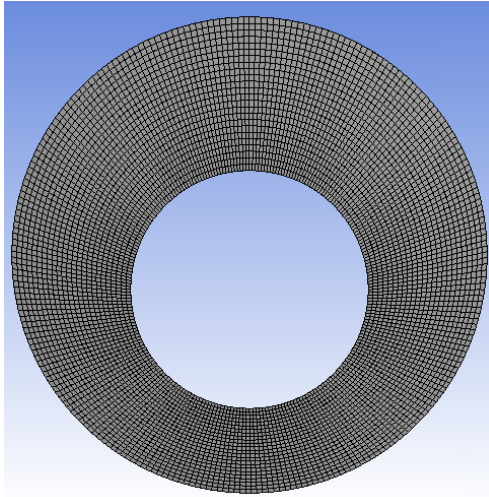


Figure 4.3 Mesh result for the model at N=1500  
Meshing Quality - 0.950

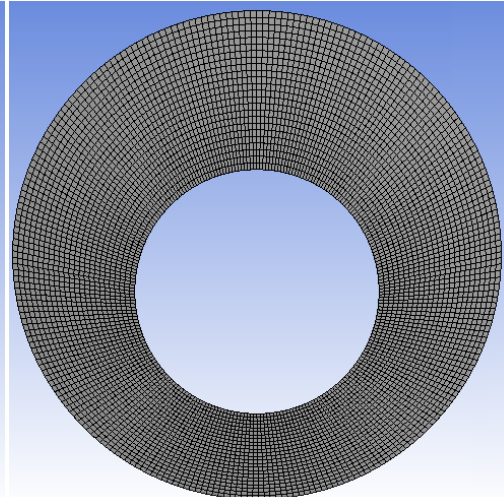


Figure 4.4 Mesh result for the model at N=1750  
Meshing Quality - 0.952

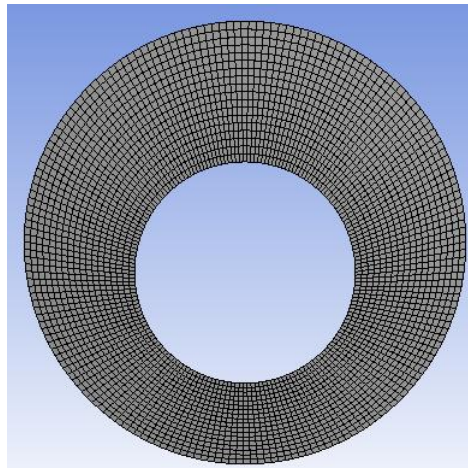


Figure 4.5 Mesh result for the model at N=2000  
Meshing Quality - 0.975

## V. Analysis and Interpretation of Data

### 5.1 Presentation of Data

In our study, after the classification of data, they are tabulated. Tabulation is the process of transferring classified data from various equations (defined in the previous chapter) to the tabular form in which they may be systematically examined. This process may be performed in a number of ways. To present data clear and concise, their tabulation is needed.

### 5.2 Technical Data Used for the Calculations

Following the ASTM D2422-97 and ISO 3448 method [9], we have taken some mineral oils for the analysis of the couette flow in the application of plain journal bearings which are used in the low speed hydraulic turbines. The mineral oils that we are using are ISO 32, ISO 46, ISO 68 and ISO 100. The properties of the above stated mineral oils are tabulated below.

#### 5.2.1 Density of Mineral Oils

Density of mineral oil, at specific temperature and atmospheric pressure, can be calculated by using experimentally-measured value of density at the temperature of  $15^{\circ}\text{C}$  and volume temperature expansion coefficient,  $\alpha_p$ , for the same temperature [6,19].

The equation used for the calculation of the density at any temperature is stated as [4,5],

$$\rho = \rho_{15} - \rho_{15}\alpha_{p15}(T - 15) = \rho_{15}(1 - 0.0007(T - 15))$$

Table 5.1 Density of Mineral Oils at  $15^{\circ}\text{C}$  and  $60^{\circ}\text{C}$

Mineral Oil	$\rho @ 15^{\circ}C$ (kg/l)	$\rho @ 60^{\circ}C$ (kg/l)
ISO 32	0.854	0.827
ISO 46	0.865	0.837
ISO 68	0.867	0.839
ISO 100	0.868	0.840

### 5.2.2 Viscosity of Mineral Oils

The values of the Kinematic Viscosity at different temperatures of various minerals oils are taken from viscosity reference table given by ASTM [9]. The Dynamic viscosity of various mineral oils is calculated by using the below mentioned formula:

$$\mu = \rho_{60} * \nu$$

**Table 5.2 Kinematic and Dynamic Viscosity of Mineral Oils**

Mineral Oil	$\nu @ 60^{\circ}C$ (cSt)	$\mu @ 60^{\circ}C$ (kg/m-s)
ISO 32	15.9	0.013
ISO 46	21.5	0.018
ISO 68	29.5	0.024
ISO 100	40.7	0.034

### 5.2.3 Tangential Velocities at different RPM

The shaft in the Plain Journal Bearing rotates with different velocities depending on the type of application in which the hydraulic turbines are used. In our study we have taken the low speed hydraulic turbines so for them the range of velocity at which the shaft rotates varies from 1000 to 2000 rpm. To calculate the tangential velocity of the shaft the following formula is used:

$$u = \omega * r = \frac{2\pi N}{60} * r$$

**Table 5.3 Angular and Tangential Velocity of the Shaft**

RPM	$\omega$ (rad/s)	r (m)	u (m/s)
1000	104.72	0.05	5.236
1250	130.9	0.05	6.545
1500	157.08	0.05	7.854
1750	183.26	0.05	9.163
2000	209.44	0.05	10.472

### 5.2.4 Thermal Conductivity and Specific Heat

Thermal conductivity and specific heat of minerals oils are generally constant when working with low temperatures [11,12,13,14,19]. Their values are tabulated below:

**Table 5.4 Thermal Conductivity and Specific Heat of Mineral Oils**

Mineral Oil	K (w/m-k)	$C_p$ (J/kg-k)
ISO 32	0.128	1942.67
ISO 46	0.129	1942.67
ISO 68	0.128	1934.3
ISO 100	0.0106	1934.3

### 5.3 Reynolds Number

The Reynold Number is calculated for various models to have a check whether the flow lies in the laminar or the turbulent regime. The Reynold Number is calculated by using the formula given below:

$$Re = \frac{\rho v d}{\mu} = \frac{v d}{\nu}$$

**Table 5.5 Reynolds Number of mineral oils at Different RPM**

Mineral Oils	RPM				
	1000	1250	1500	1750	2000
ISO 32	16.66	20.82	24.98	29.15	33.31
ISO 46	12.19	15.23	18.28	21.32	24.37
ISO 68	9.16	11.45	13.74	16.03	18.32
ISO 100	6.473	8.09	9.71	11.33	12.95

**Hypothesis 1: Our model lies in Laminar Region or not.**

$H_0: Re \leq 2100$   
 $H_1: Re > 2100$

**Table 5.6 Reynolds Number Hypothesis Testing**

Mean	Ranges		Hypothesis
	Laminar	Turbulent	
16.68	Re < 2100	Re > 5000	$H_0$ accepted

**Result:** Our study lies in Laminar Region

**5.4 Viscosity-Temperature Relation**

Following the ASTM standards [3], the Walter equation is used that defines the relation between the temperature and the kinematic viscosity. Based on the various values of the kinematic viscosity at different temperatures the values of the constants in the Walter equation are calculated for the various mineral oils used in our study. Accordingly, the equations are formed and the Viscosity- Temperature line graph is formed. The constants in the Walter equation are calculated by using the modified form of equation (24) that is given below:

$$\log\log(\nu + 0.7) = a - b \log(T)$$

**Table 5.7 Kinematic Viscosity of Mineral Oils at 30°C and 90°C**

Mineral Oil	$\nu$ @ 30°C (cSt)	$\nu$ @ 90°C (cSt)
ISO 32	49.1	7.3
ISO 46	73.2	9.3
ISO 68	113	11.9
ISO 100	173.3	15.2

Based on the data from the above table, the value of the constants is calculated.

**Table 5.8 Values of the Constants ‘a’ and ‘b’ for Walter Equation**

Mineral Oil	a	b
ISO 32	8.94	3.51
ISO 46	8.91	3.48
ISO 68	8.95	3.48
ISO 100	3.50	9.05

**5.4.1 Graph for Kinematic Viscosity Versus Temperature**

Kinematic Viscosity is calculated by using the equation (24). Using these calculated values, line graph is plotted between Kinematic Viscosity and Temperature.

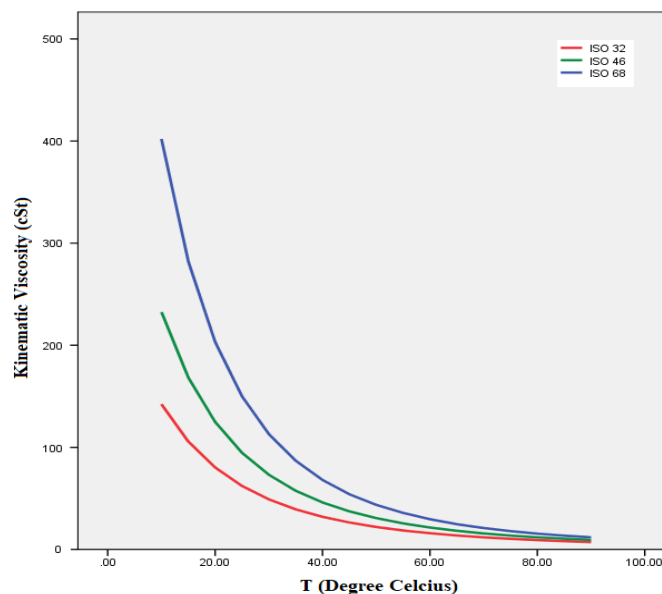


**Figure 5.1 Kinematic Viscosity Versus Temperature for Various Mineral Oils**

The above figure 5.1 shows the variation of the kinematic viscosity with the different values of temperature for various mineral oils. From the graph, it is clear that the values of the kinematic viscosity for all the mineral oils are continuously decreasing when the value of temperature is increasing. But for ISO 32, it is seen that the value of kinematic viscosity is not rapidly decreasing with the increasing value of temperature which further signifies that in ISO 32 the variation of the kinematic viscosity with temperature is minimal in ISO 32 as compared to the other various mineral oils.

**Table 5.9 Range of Kinematic Viscosity for Various Mineral Oils**

Mineral No	$r$	$\nu_{min}$	$\nu_{max}$	Range
ISO 32	-0.868	7.30	142.30	135
ISO 46	-0.854	9.30	232.50	223.20
ISO 68	-0.837	11.90	402.10	390.20

### 5.5 Viscosity Index

The Viscosity Index [2] value of mineral oils is calculated that will tell us the change in the viscosity of the oil with temperature. The Viscosity Index value is calculated by using the equation (25).

**Table 5.10 Viscosity Index of Various Mineral Oils**

Mineral Oil	$\nu @ 40^{\circ}C (cSt)$	$\nu @ 100^{\circ}C (cSt)$	VI
ISO 32	32	5.9	130.35
ISO 46	46	7.4	124.33
ISO 68	68	9.3	113.98
ISO 100	100	11.7	105.36

It is known that higher the value of Viscosity Index defines the minimum change in the viscosity with the rise of temperature in the mineral oil. ISO 32 has highest VI in all the mineral oil which means that the cohesive force is more between the particles of the ISO 32 as compared to the other mineral oils. So, ISO 32 is recommended to be used in the plain journal bearing. The effect of the viscosity and Viscosity Index in plain journal bearing has been discussed in the section 2.3 and section 2.4.

### 5.6 Temperature Ranges for ISO 32 in Ansys Workbench

The numerical simulation of the journal bearing is done for ISO 32 in Ansys Workbench. The temperature ranges are observed for different rotational speeds of the journal bearing for ISO 32 that are shown in the table 5.10:

**Table 5.11 Temperature Difference at Different RPM for ISO 32**

RPM	$T_{min} (k)$	$T_{max} (k)$	$\Delta T (K)$
1000	282.6	296.99	14.39
1250	259	300.9	41.9
1500	292.3	298.65	6.35
1750	293.3	299.9	7.6
2000	291.9	300.13	8.23

The minimum and the maximum temperature values are important to check in the plain journal bearing since the mineral oil (ISO 32) used can be operated at the temperature difference of only  $60^{\circ}C$  and hence it becomes necessary to check that whether during the operation of the plain journal bearing the temperature difference does not exceed  $60^{\circ}C$ , especially in the plain journal bearings where the danger of the breakage of the molecules is always there that can significantly increase the temperature within the system. As the above tabulated values of the temperature difference are all less than  $60^{\circ}C$ , hence ISO 32 can be used in the plain journal bearing. The visuals (pictures) obtained in the Ansys for the ISO 32 at different rotational speeds of the shaft are shown from figure 5.2 to figure 5.6:

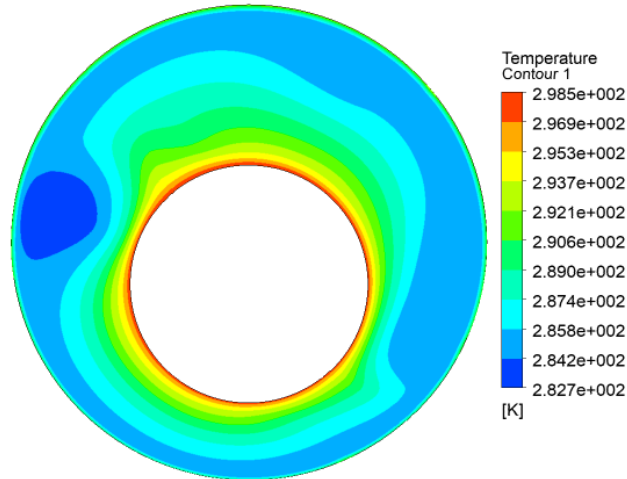


**Figure 5.2 Temperature Contour of ISO 32 at N=1000 rpm**

The above fig 5.2 shows the temperature contours of ISO 32 at the rotational speed of the shaft of 1000 rpm. It is observed that the temperature variation for the above model will be 14.39 K, with the maximum temperature occurring at the shaft and the minimum temperature occurring at the location around the journal. There is a thin film of maximum temperature around the shaft and the thickness of the film is very small. This will be mainly due to the low rotational speed of the shaft. The heat must be transferred from the shaft to the journal.

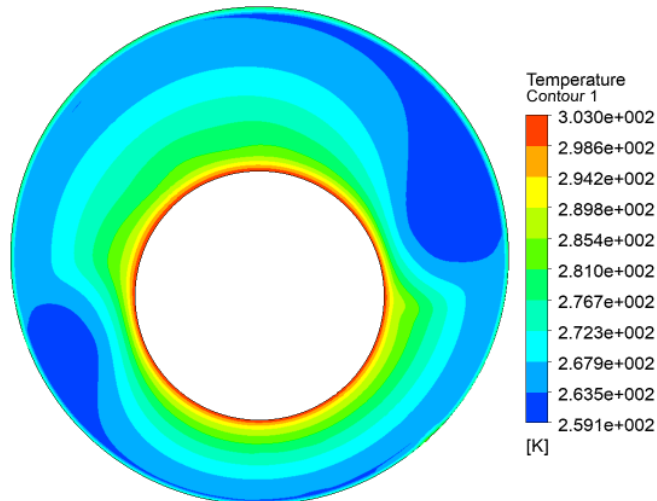


**Figure 5.3 Temperature Contour of ISO 32 at N=1250 rpm**

The above fig 5.3 shows the temperature contours of ISO 32 at the rotational speed of the shaft of 1250 rpm. It is observed that the temperature variation for the above model will be 41.9 K, with the maximum temperature occurring at the shaft and the minimum temperature occurring at the location around the journal. There is a film of maximum temperature around the shaft and the thickness of the film is some large as compared to the thickness of the film observed at N=1000 rpm.

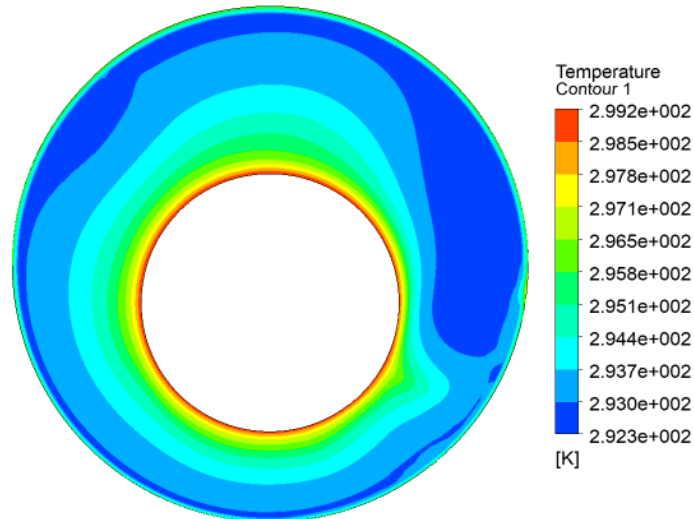


Figure 5.4 Temperature Contour of ISO 32 at N=1500 rpm

The above fig 5.4 shows the temperature contours of ISO 32 at the rotational speed of the shaft of 1500 rpm. It is observed that the temperature variation for the above model will be 6.35 K, with the maximum temperature occurring at the shaft and the minimum temperature occurring at the location around the journal. There is a film of maximum temperature around the shaft and the thickness of the film is some large as compared to the thickness of the film observed at N=1250 rpm.

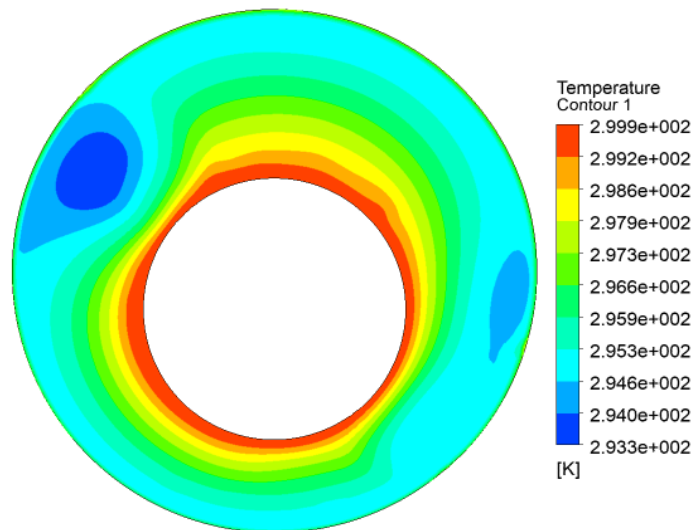
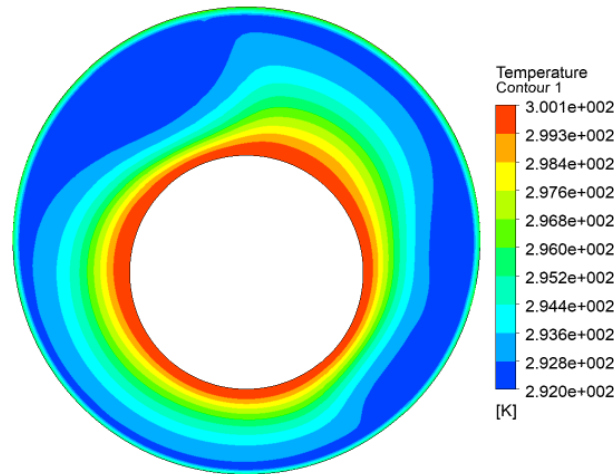


Figure 5.5 Temperature Contour of ISO 32 at N=1750 rpm

The above fig 5.5 shows the temperature contours of ISO 32 at the rotational speed of the shaft of 1750 rpm. It is observed that the temperature variation for the above model will be 7.6 K, with the maximum temperature occurring at the shaft and the minimum temperature occurring at the location around the journal. There is a film of maximum temperature around the shaft and the thickness of the film very large as compared to the other thickness of the film that were observed at N= 1000, N= 1250 and N=1500.



**Figure 5.6 Temperature Contour of ISO 32 at N=2000 rpm**

The above fig 5.6 shows the temperature contours of ISO 32 at the rotational speed of the shaft of 2000 rpm. It is observed that the temperature variation for the above model will be 7.6 K, with the maximum temperature occurring at the shaft and the minimum temperature occurring at the location around the journal. There is a film of maximum temperature around the shaft and the thickness of the film is very large as compared to the other thickness of the film that were observed at N= 1000, N= 1250, N=1500 and N=1750. This shows that as the rotational speed of the shaft increases, the temperature increases in the plain journal bearing and the heat should be dissipated from the shaft to the outside area.

**5.7 Maximum Heat Flux**

The maximum Heat Flux that can occur in our model of couetteflow at a mean temperature of 60°C can be calculated by using the equation (19) and equation (21) for the top and the bottom plates for all the mineral oils. The direction of the heat flux depends on the value of the brinkmannnumber (Br) which can be calculated by using the equation (22). The value of the heat flux and the brinkmannnumber are useful in deciding the best possible mineral oil that can be used for the purpose of the plain journal bearing used in the application of the low speed hydraulic turbines.

**Table 5.12 Brinkmann Number and Maximum Heat Flux of Mineral Oils at N=1000 rpm**

Mineral Oil	Br	$q_{max\ Top\ Plate}\ (W/m^2)$	$q_{max\ Bottom\ Plate}\ (W/m^2)$
ISO 32	0.046	150.04	157.16
ISO 46	0.064	149.87	159.73
ISO 68	0.086	147.03	160.17
ISO 100	1.464	3.41	22.03

**Table 5.13 Brinkmann Number and Maximum Heat flux of Mineral Oils at N=1250 rpm**

Mineral Oil	Br	$q_{max\ Top\ Plate}\ (W/m^2)$	$q_{max\ Bottom\ Plate}\ (W/m^2)$
ISO 32	0.072	148.04	159.16
ISO 46	0.1	147.1	162.5
ISO 68	0.134	143.33	163.87
ISO 100	2.288	-1.83	27.27

**Table 5.14 Brinkmann Number and Maximum Heat flux of Mineral Oils at N=1500 rpm**

Mineral Oil	Br	$q_{max\ Top\ Plate}\ (W/m^2)$	$q_{max\ Bottom\ Plate}\ (W/m^2)$
ISO 32	0.104	145.59	161.61
ISO 46	0.143	143.71	165.89
ISO 68	0.193	138.81	168.39
ISO 100	3.294	-8.23	33.67

**Table 5.15 Brinkmann Number and Maximum Heat flux of Mineral Oils at N=1750 rpm**

Mineral Oil	Br	$q_{max\ Top\ Plate}\ (W/m^2)$	$q_{max\ Bottom\ Plate}\ (W/m^2)$
ISO 32	0.142	142.7	164.5
ISO 46	0.195	139.7	169.9
ISO 68	0.262	133.47	173.73
ISO 100	4.484	-15.8	41.24

**Table 5.16 Brinkmann Number and Maximum Heat flux of Mineral Oils at N=2000 rpm**

Mineral Oil	Br	$q_{max\ Top\ Plate}\ (W/m^2)$	$q_{max\ Bottom\ Plate}\ (W/m^2)$
ISO 32	0.185	139.36	167.84
ISO 46	0.255	135.08	174.52
ISO 68	0.342	127.31	179.89
ISO 100	5.857	-24.53	49.97

From the above tabulated values of the heat flux for different mineral oils it is observed that the heat flux at the top plate is maximum for ISO 32 which signifies that ISO 32 will be able to remove the maximum heat from the system thus acting as a coolant in a more effective way than the other mineral oils. Regarding the Bottom plate the heat flux values are less for ISO 32 which signifies that the heat dissipation will be the least in ISO 32 as compared to the other mineral oils, which further proves that ISO 32 will be the best mineral oil to be used. This can be proved also statistically by calculating the standard deviation of the heat flux values for all the mineral oils. So standard deviation is calculated for different mineral oil using SPSS software.

**Table 5.17 Standard Deviation of the Heat Flux for Various Mineral Oils**

Mineral oil	Mean Heat Flux		Standard Deviation	
	Top plate	Bottom plate	Top plate	Bottom plate
ISO 32	145.26	161.94	3.33	3.33
ISO 46	143.26	166.34	4.6	4.6
ISO 68	138.21	168.99	6.14	6.14
ISO 100	-9.04	34.53	8.77	8.701

As much as, the heat flux value will deviate from its mean value, the standard deviation will increase. The higher value of the standard deviation shows lesser the heat dissipation of the heat flux from the plain journal bearing. From the above calculated values of the standard deviation for the top plate and the bottom plate it is clear to note that the value of the standard deviation is less in ISO 32 as compared to the other mineral oils. Hence from the statistical tools as well it is clear that the ISO 32 is clearly the best mineral oil to be used for our study of the model.

**5.7.1 Graphs of Brinkmann Number Versus RPM**

Brinkmann Number is calculated by using the equation (22) and values are tabulated in section (5.7). Using these calculated values, line graph is plotted between brinkmannnumber and rotational speed of the journal bearing.

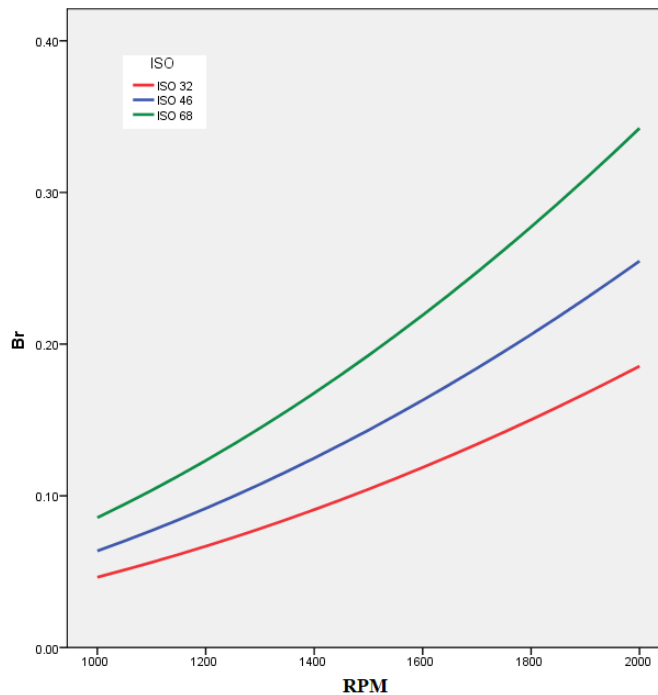


**Figure 5.7 Brinkmann Number Versus RPM for Various Mineral Oils**

The above figure 5.7 shows the variation of the brinkmannnumber with the different values of the rotational speed of the shaft for various mineral oils. From the graph, it is clear that the values of the brinkmannnumber for all the mineral oils are continuously increasing when the value of the rotational speed of the shaft is increasing. But, for ISO 32 the values of brinkmannnumber are not rapidly increasing with the increasing value of the rotational speed which further signifies that the viscous dissipation in ISO 32 will be the least among the three stated mineral oils. Hence, for the present study ISO 32 will be the best mineral oil to be used.

**Table 5.18 Range of Brinkmann Number for Various Mineral Oils**

Mineral No	r	$Br_{min}$	$Br_{max}$	Range
ISO 32	0.996	0.0464	0.1854	0.1391
ISO 46	0.996	0.0637	0.2548	0.1911
ISO 68	0.996	0.2568	0.3423	0.2568

**5.7.2 Heat Flux Versus RPM**

Heat flux is calculated by using the equation (19) and values are tabulated in section (5.7). Using these calculated values, line graph is plotted between heat flux and rotational speed of the journal bearing.

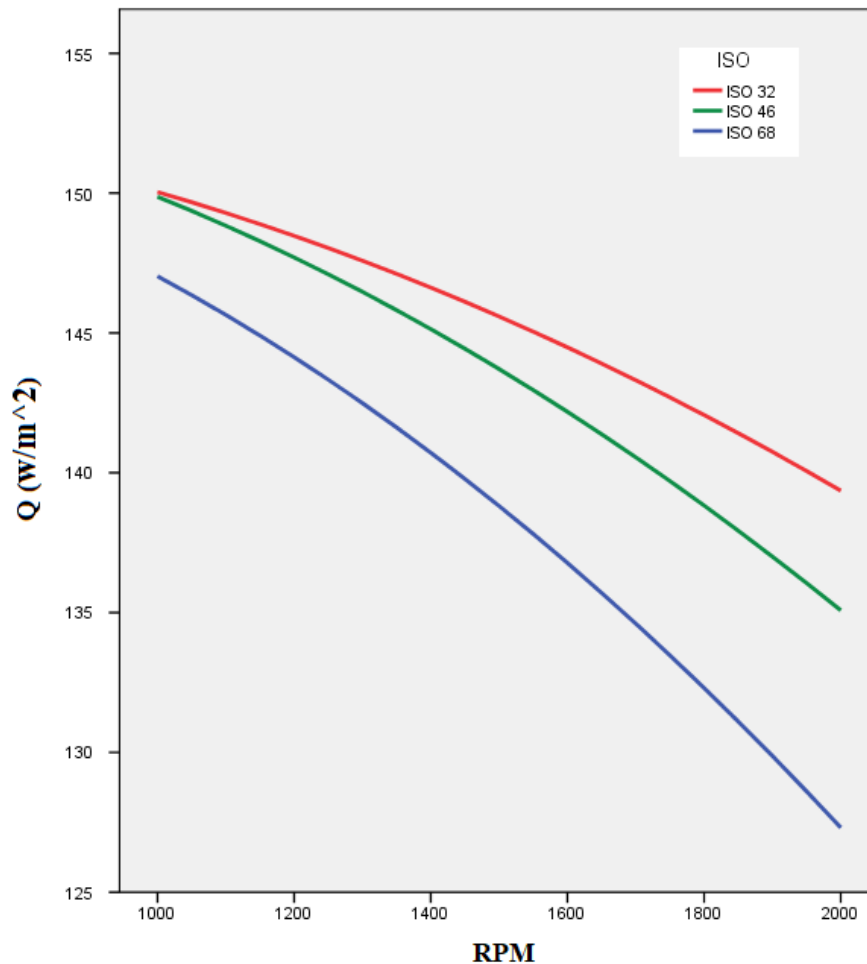


**Figure 5.8 Heat Flux Versus RPM for Various Mineral Oils**

The above figure 5.8 shows the variation of the heat flux with the different values of the rotational speed of the shaft for various mineral oils. From the graph, it is clear that the values of the heat flux for all the mineral oils are continuously decreasing when the value of the rotational speed of the shaft is increasing. But, for ISO 32 it is seen that the value of heat flux is not rapidly decreasing with the increasing value of the rotational speed which further signifies that with the increasing rotational speed of the shaft, ISO 32 will be able to extract the largest amount of heat from the system, which is one of the important consideration in selecting the best mineral oil for the study of the plain journal bearing.

**Table 5.19 Range of Heat Flux for Various Mineral Oils**

Mineral No	r	$q_{min}$	$q_{max}$	Range
ISO 32	-0.996	139.36	150.04	10.68
ISO 46	-0.996	135.08	149.87	14.79
ISO 68	-0.996	127.31	147.03	19.72

**5.7.3 Graph of Heat Flux Versus Vertical Distance for ISO 32**

Heat flux is calculated by using the equation (18), then line graph is plotted between the heat flux and the vertical distance along the y direction.

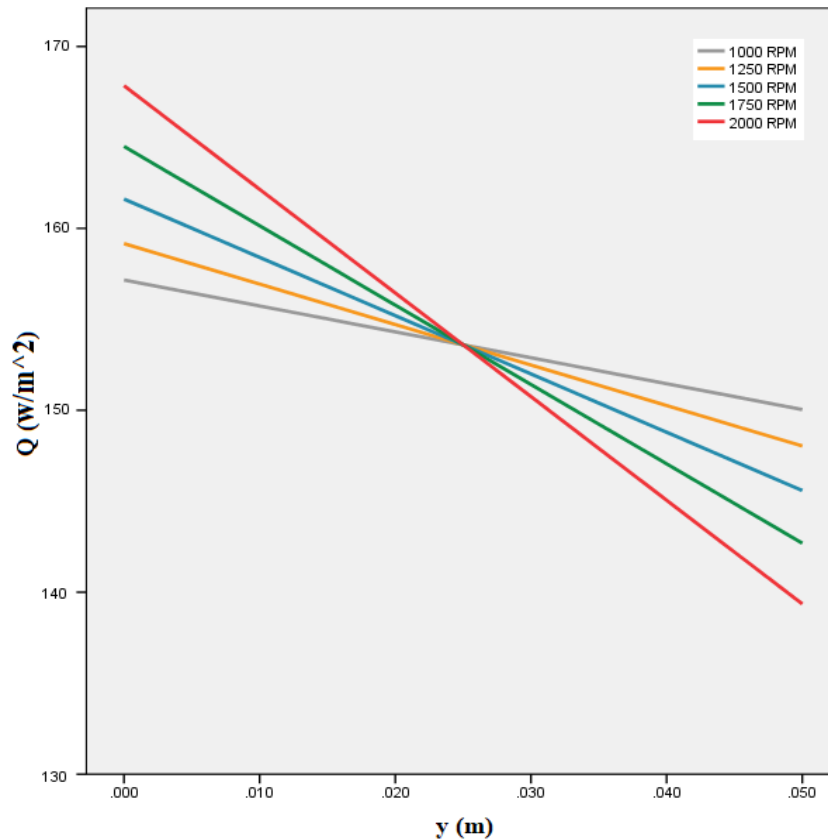


**Figure 5.9 Heat Flux Versus Vertical Distance for ISO 32 at  $\Delta T = 60^\circ C$**

The above figure 5.9 shows the variation of the heat flux with the various values of vertical distance for ISO 32 at the range of rotational speed of the shaft as 1000-2000 rpm. From the above graph it is clearly seen that the variation in the heat flux is maximum for  $N=2000$  rpm and it decreases when the rotational speed decreases which further signifies that the heat dissipation increases when the rotational speed increases.

**Table 5.20 Range of Heat Flux at Different RPM for ISO 32**

RPM	$q_{min}$	$q_{max}$	Range
1000	150.04	157.16	7.12
1250	148.04	159.16	11.13
1500	145.59	161.61	16.02
1750	142.70	164.50	21.81
2000	139.36	167.84	28.48

**5.8 Analytical Results of Heat Flux for ISO 32**

The maximum value of the heat flux is calculated in the section (5.7) by using the mean temperature of  $60^\circ C$ . From the section (5.7), ISO 32 was proved to be the best optimal mineral oil. So now the values of the heat flux are calculated using the temperature difference values shown in section 5.6 that were found in the analytical results of ISO 32. The values of the heat flux are tabulated below in table 5.17:

**Table 5.21 Brinkmann Number and Heat Flux at Different RPM of ISO 32**

RPM	$\Delta T$ (K)	Br	$q_{Top\ Plate}$ (W/m <sup>2</sup> )	$q_{Bottom\ Plate}$ (W/m <sup>2</sup> )
1000	14.39	0.193	33.29	40.4
1250	41.9	0.104	101.7	112.83
1500	6.35	0.986	8.245	24.267
1750	7.6	1.12	8.55	30.36
2000	8.23	1.352	6.827	35.31

**5.8.1 Comparison of Quantitative and Analytical Heat Flux results of ISO 32**

The quantitative heat flux values are calculated in section 5.7 and analytical heat flux values are calculated in section 5.8. SPSS software is used to compare the results. Paired Sample T Test has been applied to compare the variation of the quantitative and the analytical heat flux results of ISO 32. Hypothesis testing is done at the significance level of 95% and null hypothesis and alternate hypotheses are formed.

**Hypothesis 2: Analytical Heat Flux values are less than or equal to Quantitative Heat Flux values**

$H_0: \mu_{hf1} \leq \mu_{hf2}$

$H_1: \mu_{hf1} > \mu_{hf2}$

**Table 5.22 Hypothesis Testing of Heat Flux for ISO 32**

	Mean	Mean Difference	Hypothesis
$q_{max(top)}$	$\mu_{hf2} = 145.14$	113.43	$\mu_{hf1} < \mu_{hf2}$ $H_0$ accepted
$q_{Top}$	$\mu_{hf1} = 31.72$		
$q_{max(bottom)}$	$\mu_{hf2} = 162.06$	113.43	$\mu_{hf1} < \mu_{hf2}$ $H_0$ accepted
$q_{bottom}$	$\mu_{hf1} = 48.63$		

Hence analytical heat flux results of ISO 32 are less than quantitative heat flux results.

**5.9 Maximum Entropy Generation**

Based on the Second Law of thermodynamics the maximum local volumetric rate of entropy generation is calculated at the top and the bottom plate by using the equation (23) for all the mineral oils. The value of the entropy generation is useful in finding the best possible lubricant for the analysis of the model as the entropy generation leads to the analysis of the irreversibility occurring within the system and hence the entropy generation becomes helpful while dealing with the heat transfer problems.

**Table 5.23 Entropy Generation of Mineral Oils at N=1000 rpm**

Mineral Oil	$S_{G\ max(Top\ Plate)}$ (W. m <sup>-3</sup> . k <sup>-1</sup> )	$S_{G\ max(Bottom\ Plate)}$ (W. m <sup>-3</sup> . k <sup>-1</sup> )
ISO 32	2.39	2.57
ISO 46	2.55	2.81
ISO 68	2.74	3.09
ISO 100	1.17	1.63

**Table 5.24 Entropy Generation of Mineral Oils at N=1250 rpm**

Mineral Oil	$S_{G\ max(Top\ Plate)}$ (W. m <sup>-3</sup> . k <sup>-1</sup> )	$S_{G\ max(Bottom\ Plate)}$ (W. m <sup>-3</sup> . k <sup>-1</sup> )
ISO 32	2.6	2.89
ISO 46	2.84	3.25
ISO 68	3.15	3.71
ISO 100	1.81	2.52

**Table 5.25 Entropy Generation of Mineral Oils at N=1500 rpm**

Mineral Oil	$S_{G\ max(Top\ Plate)}$ (W. m <sup>-3</sup> . k <sup>-1</sup> )	$S_{G\ max(Bottom\ Plate)}$ (W. m <sup>-3</sup> . k <sup>-1</sup> )
ISO 32	2.86	3.28
ISO 46	3.21	3.79
ISO 68	3.66	4.46
ISO 100	2.65	3.68

**Table 5.26 Entropy Generation of Mineral Oils at N=1750 rpm**

Mineral Oil	$S_{G\ max(Top\ Plate)}$ (W. m <sup>-3</sup> . k <sup>-1</sup> )	$S_{G\ max(Bottom\ Plate)}$ (W. m <sup>-3</sup> . k <sup>-1</sup> )
ISO 32	3.17	3.74
ISO 46	3.64	4.43

ISO 68	4.27	5.36
ISO 100	3.75	5.15

**Table 5.27 Entropy Generation of Mineral Oils at N=2000 rpm**

Mineral Oil	$S_{G \max(\text{Top Plate})} (\text{W} \cdot \text{m}^{-3} \cdot \text{k}^{-1})$	$S_{G \max(\text{Bottom Plate})} (\text{W} \cdot \text{m}^{-3} \cdot \text{k}^{-1})$
ISO 32	3.53	4.28
ISO 46	4.14	5.17
ISO 68	4.97	6.4
ISO 100	5.14	6.97

From the above tabulated values of the entropy for different mineral oils it is observed that the entropy at the top plate is less for ISO 32 which signifies that in case of ISO 32 the irreversibility in the system will be least which is the most important parameter for the system. Regarding the bottom plate the entropy values are less for ISO 32 which signifies that the irreversibility will be the least in ISO 32 as compared to the other mineral oils, which further proves that ISO 32 will be the best mineral oil to be used. This can be proved also statistically by calculating the standard deviation of the entropy generation values for all the mineral oils. So standard deviation is calculated for different mineral oil using SPSS software.

**Table 5.28 Standard Deviation of the Entropy for Various Mineral Oils**

Mineral oil	Mean Entropy		Standard Deviation	
	Top plate	Bottom plate	Top plate	Bottom plate
ISO 32	2.89	3.33	0.36	0.53
ISO 46	3.26	3.86	0.49	0.74
ISO 68	3.74	4.57	0.69	1.03
ISO 100	2.84	3.9	1.23	1.66

As much as, the entropy generation values will deviate from its mean value, the standard deviation will increase. The higher value of the standard deviation shows lesser the irreversibility in the plain journal bearing. From the above calculated values of the standard deviation for the top plate and the bottom plate it is clear to note that the value of the standard deviation is less in ISO 32 as compared to the other mineral oils. Hence from the statistical tools as well it is clear that the ISO 32 is clearly the best mineral oil to be used for our study of the model.

**5.9.1 Entropy Versus RPM**

Entropy is calculated by using the equation (23) and values are tabulated in section (5.9). Using these calculated values, line graph is plotted between entropy and rotational speed of the journal bearing.

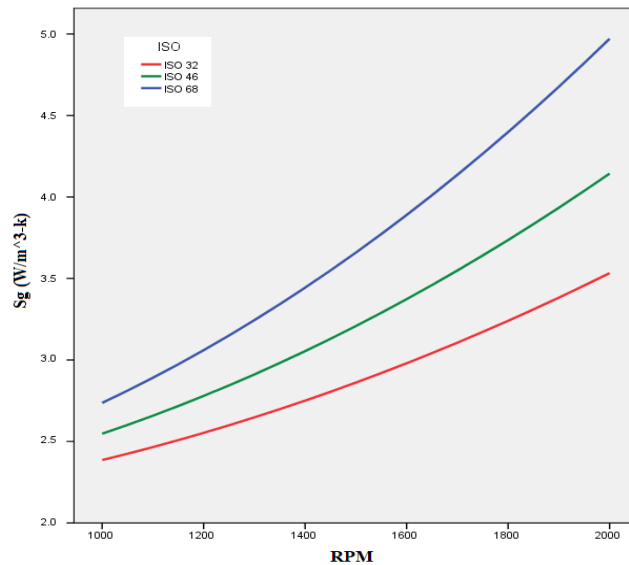


**Figure 5.10 Entropy Versus RPM for Various Mineral Oils**

The above figure 5.10 shows the variation of the entropy with the different values of the rotational speed of the shaft for various mineral oils. From the graph, it is clear that the values of the entropy for all the

mineral oils are continuously increasing when the value of the rotational speed of the shaft is increasing. But, for ISO 32 it is seen that the value of entropy is not rapidly increasing with the increasing value of the rotational speed which further signifies that with the increasing value of the rotational speed of the shaft the volumetric rate of entropy generation will be the least in the case of ISO 32 among all the various mineral oils used.

**Table 5.29 Range of Entropy for Various Mineral Oils**

Mineral No	r	$Sg_{min}$	$Sg_{max}$	Range
ISO 32	0.996	2.39	3.53	1.15
ISO 46	0.996	2.55	4.14	1.60
ISO 68	0.996	2.74	4.97	2.23

**5.9.2 Entropy versus Vertical Distance for ISO 32**

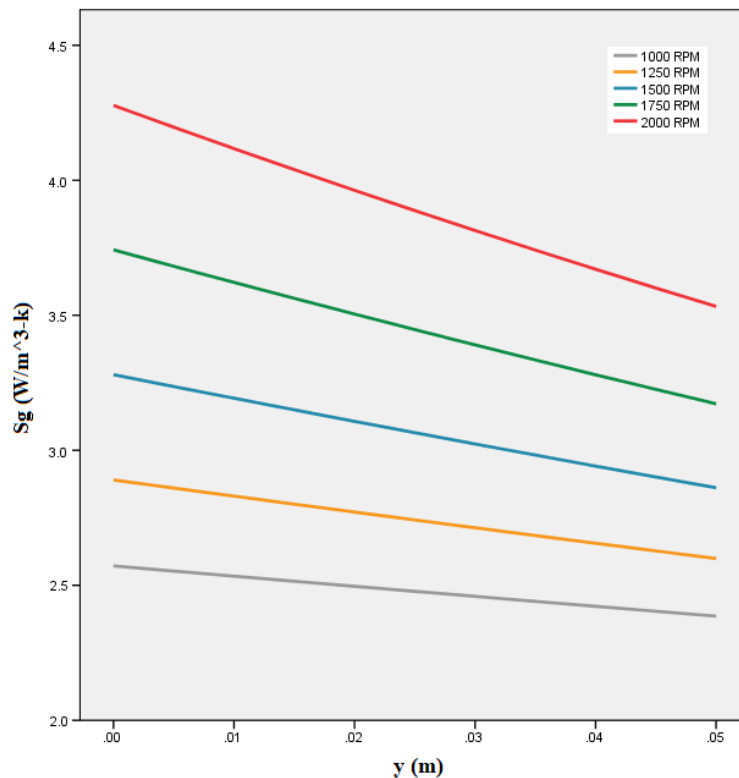


**Figure 5.11 Entropy versus Vertical Distance for ISO 32 at  $\Delta T = 60^{\circ}C$**

The above figure 5.11 shows the variation of the entropy with the various values of vertical distance for ISO 32 at the range of rotational speed of the shaft as 1000-2000 rpm. From the above graph it is clearly seen that the variation in the entropy is maximum for  $N=2000$  rpm and it decreases when the rotational speed decreases which further signifies that the irreversibility increases when the rotational speed increases.

**Table 5.30 Range of Entropy at Different RPM for ISO 32**

RPM	$Sg_{min}$	$Sg_{max}$	Range
1000	2.39	2.57	0.19
1250	2.60	2.89	0.29
1500	2.86	3.28	0.42
1750	3.17	3.74	0.57
2000	3.53	4.28	0.74

**5.10 Analytical Results of Entropy Generation for ISO 32**

The maximum values of the entropy generation are calculated in the section (5.9) by using the mean temperature of  $60^{\circ}C$ . From the section (5.9), ISO 32 was proved to be the best optimal mineral oil. So now the values of the entropy are calculated using the temperature difference shown in section 5.6 that were found in the analytical results of ISO 32. The values of the entropy are tabulated below in the table

**Table 5.31 Entropy Generation at Different RPM for ISO 32**

RPM	$\Delta T$ (K)	$S_G$ (Top Plate) (W.m <sup>-3</sup> .k <sup>-1</sup> )	$S_G$ (Bottom Plate) (W.m <sup>-3</sup> .k <sup>-1</sup> )
1000	14.39	0.61	0.66
1250	41.9	2.06	2.34
1500	6.35	1.1	1.15
1750	7.6	1.49	1.57
2000	8.23	1.96	2.07

**5.10.1 Comparison of Quantitative and Analytical Entropy results of ISO 32**

The quantitative entropy generation values are calculated in section 5.9 and analytical entropy generation values are calculated in section 5.10. SPSS software is used to compare the results. Paired Sample T Test has been applied to compare the variation of the quantitative and the analytical entropy results of ISO 32. Hypothesis Testing is done at the significance level of 95% and null hypothesis and alternate hypotheses are formed.

**Hypothesis 3: Analytical Entropy values are less than or equal to Quantitative Entropy values**

$H_0: \mu_{e1} \leq \mu_{e2}$

$H_{11}: \mu_{e1} > \mu_{e2}$

**Table 5.32 Hypothesis Testing of Entropy for ISO 32**

	Mean	Mean Difference	Hypothesis
$S_G$ max(Top Plate)	$\mu_{e2} = 2.91$	1.47	$\mu_{e1} < \mu_{e2}$ $H_0$ accepted
$S_G$ (Top Plate)	$\mu_{e1} = 1.44$		
$S_G$ max(bottom Plate)	$\mu_{e2} = 3.35$	1.79	$\mu_{e1} < \mu_{e2}$ $H_0$ accepted
$S_G$ (bottom Plate)	$\mu_{e1} = 1.56$		

Hence analytical entropy results of ISO 32 are less than quantitative entropy results.

**5.11 Results and Discussion**

**5.11.1 Quantitative Results for Various Mineral Oils**

The journal bearing used for our study is the plain journal bearing. It has two components, one representing the shaft and the other is the journal that represents the stationary component. Between the two parts there is the lubricant that is supplied through openings, which emerge in an axial groove. The technical data used are given in the section 5.2.

From the calculated values of the Reynold’s number for the rpm range of 1000-2000 for the model of the Couette flow in the section (5.3), it has been observed that all the values of the Reynold’s Number are less than 2100, which signifies that the flow lies in the laminar regime and hence there is no turbulence within the flow.

From the calculated values of the Viscosity Index in the section (5.6), it has been observed that the value of the viscosity index is more in ISO 32 as compared with the other mineral oils, which signifies that the variation of the viscosity with temperature will be the least in ISO 32 as compared with other mineral oils. This is an important result since it is recommended that the variation in viscosity must be less with temperature for the stable conditions to be achieved.

From the heat flux equation derived in the section (3.3.1), it has been observed that the direction of the heat flux depends on the value of the Brinkmann Number. The following cases are possible:

- When ( $Br > 2$ ), the heat flux in this case will be positive and the heat flows from the lower plate to the upper plate even though the upper plate is at the higher temperature and this will violate the second law of thermodynamics. So actually, in this case what happens is that due to viscous dissipation locally the temperature near the upper plate will become more than  $T_1$  and hence heat transfer takes place from the lower plate to the upper plate. Here the viscous dissipation basically acts as a heat source.
- When ( $Br = 2$ ), the heat flux in this case becomes zero. Here the upper plate acts as an insulator. Hence despite a temperature gradient being present between the two plates there is actually no heat transfer. This is because the temperature difference created due to the viscous dissipation is exactly nullified by the conduction between the two plates.
- When ( $Br < 2$ ), the heat flux in this case will be negative and the heat flows from the upper plate to the lower plate.

From the calculated values of the maximum heat flux for the top as well as the bottom plate in the section (5.8), it is observed that the values of the Brinkmann Number for ISO 32, ISO 46 and ISO 68 are less

than 2 for the rpm range of 1000 to 2000 rpm and hence the heat flux will be negative and the heat flows from the upper plate to the lower plate. But for ISO 100 the values of the brinkmannnumber are greater than 2 and hence the heat generation will be there due to the viscous dissipation and hence ISO 100 will not be used as a lubricant for rpm range of 1000-2000 rpm.

From the entropy equation mentioned in the section (3.4.1), it has been observed that the volumetric rate of entropy generation in the model is due to the heat transfer within the two plates and due to the fluid friction. The factor that dominates can be calculated by using the equation given in section (3.4.2). The entropy is generated from the irreversibility in the system and hence the lesser the entropy the lesser will be the irreversibility.

From the calculated values of the maximum entropy generated in the section (5.10), it is observed that the values of the entropy generation in the top as well as the bottom plate is less for ISO 32 as compared with other mineral oils for the rpm range of 1000-2000, which signifies that the irreversibility for the model will be the least when we are using ISO 32 as our mineral oil. Though the entropy generation for ISO 100 is less for rpm of 1000 and 1250 than ISO 32 but for another rpm greater than 1250 it is more than ISO 32. Thus, when we take the mean of the results as done in the section (5.10), it is seen that the standard deviation for ISO 32 is the least as compared to the other mineral oils. Hence, for our study ISO 32 is the best mineral oil to be used.

### **5.11.2 Analytical Simulation Results of ISO 32**

The above-mentioned quantitative results are found out at the temperature difference of 60°C. From the quantitative results it is clear that the ISO 32 will be the best mineral oil to be used in our model as compared to the other mineral oils.

Now, the plain journal bearing is modelled in ANSYS Workbench by taking the ISO 32 as our mineral oil and taking the respective eccentricity at various rpm. The temperature range is found out for the model with ISO 32 as the mineral oil. From the temperature ranges found out from the Ansys the heat flux is calculated in the section (5.9) and the entropy values are calculated in the section (5.11).

From the above results, it is observed that the temperature variation for the plain journal bearing with ISO 32 as our mineral oil is less when the rotational speed of the shaft is greater than 1250 rpm. Hence, it can be concluded that the ISO 32 works best when the rotational speed of the shaft is greater than 1250 rpm.

From the analytical results of the temperature range for ISO 32 at different rpm the heat flux are calculated in the section (5.9) and from that results also it is observed that the value of the brinkmannnumber is less than 2 and hence the direction of the heat flux will be from the shaft to the journal, which is the required condition for our study. Hence, ISO 32 also proved to be the best mineral oil to be used for our study analytically as well.

Further it has been observed that the viscous dissipation for the ISO 32 keeps on increasing as the rotational speed of the shaft keeps on increasing. Hence with greater rpm the fluid friction keeps on increasing for ISO 32.

From the analytical results of the temperature range for ISO 32 at different rpm the entropy are calculated in the section (5.11) and from that results also it is observed that the value of the Entropy is less than that of the maximum entropy calculated in the section (5.10) which signifies that the ISO 32 can be used in the plain journal bearing for the rpm range of 1000-2000.

Further it has been observed that the value of the entropy keeps on increasing as the rotational speed of the shaft is increasing which further signifies that the irreversibility keeps on increasing with the rotational speed of the shaft.

## **VI. Conclusions**

### **6.1 Hypothesis Results of the Study**

#### **1. Our model lies in laminar region or not.**

**Result:** Means of the Reynold Number values were calculated and then they were compared the ranges of the Reynold Number that defines the region. It was concluded that our study lies in the laminar region.

#### **2. Analytical Heat Flux vales are less than or equal to Quantitative Heat Flux values.**

**Result:** To compare the analytical and quantitative heat flux results, Paired T test (parametric test) was applied and it was found that analytical heat flux values were less than quantitative heat flux values.

#### **3. Analytical Entropy vales are less than or equal to Quantitative Entropy values.**

**Result:** To compare the analytical and quantitative entropy results, Paired T test (parametric test) was applied and it was found that analytical entropy values were less than quantitative entropy values.

### **6.2 Conclusions**

In our study, plain journal bearing is modelled as the plain couetteflow. The conclusions of our study are:

- Our model lies in the laminar region as the value of Reynold Number is less than 2100.
- The Viscosity Index is maximum for the ISO 32 among all the mineral oils which shows very less change in the viscosity with the increase in the temperature.
- Among the all mineral oils (ISO32, ISO 46, ISO 68 and ISO 100), heat flux in the model is maximum for the ISO 32 at all the stated rotational speeds.
- Among the all mineral oils (ISO32, ISO 46, ISO 68 and ISO 100), the irreversibility in the model is least for the ISO 32 at all the stated rotational speeds.

Hence, ISO 32 is proved to be the optical mineral oil among all the mineral oils. ISO 32 is providing best results at every rotational speed of the shaft i.e. 1000 to 2000 rpm.

### **6.3 Applications of the Study**

- The model of the couette flow can be used for the study of the plain journal bearing as is done in the previous sections. This can be proved when we study the model of the plain journal bearings in which we can see that there is a rotating element, shaft and the fixed element, journal. Similarly, in the couette flow there are two parallel plates out of which one is moving and the other one is fixed. The gap between the journal and the shaft is very less and hence the curvature effects can be ignored. Hence, the plain journal bearing can be studied as a classical example of the Couette flow.
- Another application of the model can be the flow in the rectangular ducts used in the heating ventilation air conditioning systems. The model can be used with a little consideration that while deriving the heat flux equations the boundary condition can be changed and then by applying them the equations can be derived for further usage. Hence the model can be applied for this application as well.

### **6.4 Limitations of the Study**

In our study, certain limitations are there, such as:

- Steady state is considered
- Newtonian fluids are considered
- External environment parameters (temperature, pressure, speed of the air etc.) that can affect the working of the plain journal bearing are not considered here.
- Selection of best mineral oil is done only out of four mineral oil as there are many numbers of mineral oils to be used in bearing.
- Temperature Viscosity relation is studied by following only Walter equation as there are many other equations that defines same relation while considering the different factors.
- We have used only non Stokesian fluids in our study.
- We have considered constant viscosity and constant thermal conductivity during the calculation of the heat flux and entropy.

### **6.5 Suggestions for Further Study**

- Transient state also can be considered during the study.
- Non-Newtonian fluids also can be considered during the study.
- External environment affect also can be considered during the working of the plain journal bearing.
- Equations like Vogel equation, Arrhenius equation etc also can be considered to study the relation of the viscosity and temperature.
- Stokesian fluids also can be considered during the study.
- Varying viscosity and thermal conductivity also can be considered during the calculation of the heat flux and entropy.

## **References**

- [1]. AbdessamedNessil, Salah Larbi, HaceneBelhaneche and MaamarMalk, "Journal Bearing Lubrication Aspect Analysis Using Non-Newtonian Fluids", Hindawi Publishing Corporation, Advances in Tribology, 2013
- [2]. ASTM D2270 "Standard Practice for Calculating Viscosity Index from Kinematic Viscosity at 40 and 100°C," ASTM International, Conshohocken, Pa., 2010.
- [3]. ASTM D341 "Standard Test Method for Viscosity-Temperature Charts for Liquified Petroleum Products", ASTM International, Conshohocken, Pa., 2010.
- [4]. Convections, "Use of Conservation Equations", www.nptel.com
- [5]. Dana J. Salamone, "Journal Bearing Design Types and their applications to Turbomachinery", Centritech Corporation, Houston, Texas
- [6]. Darko Knezevic and Vladimir Savic, "Mathematical Modelling of Changing of Dynamic Viscosity, as a function of Temperature and Pressure", Vol 4, pp. 27-34, 2006.

- [7]. Denis R. Garner and Anthony J. Leopard, "Temperature Measurements in Fluid Film Bearings", the Glacier Metal Company Limited, England
- [8]. "Heat Generation and Temperature rise", pp. 161-162, 2008
- [9]. ISO 3448, "Viscosity Reference Table", ISO 5-9, www.iso.org, 2004.
- [10]. Malcolm E. Leader, "Understanding Journal Bearings", Applied Machinery Dynamic Co., Colorado.
- [11]. "MOL Thermol 32", Heat Transfer Oil, MOL-LUB Ltd, 2018.
- [12]. "MOL Thermol 46", Heat Transfer Oil, MOL-LUB Ltd, 2018.
- [13]. "MOL Thermol 68", Heat Transfer Oil, MOL-LUB Ltd, 2018.
- [14]. "MOL Thermol 100", Heat Transfer Oil, MOL-LUB Ltd, 2018.
- [15]. Nehal S. Ahmed and Amal M. Nassar, "Lubrication and Lubricants", Egyptian Petroleum Research Institute, Egypt, 2013.
- [16]. Sarah Isert, "Heat Transfer through a Rotating Ball Bearing at Low Angular Velocities", Utah State University
- [17]. Shohel Mahmud, Roydon Andrew Fraser, "Thermodynamic Analysis of flow and heat transfer inside channel with two parallel plates", University of Waterloo, 2001.
- [18]. "SPSS for Windows Step by Step By Darren George and Paul Malley", Pearson
- [19]. Trojan Aw Series, "Anti Wear Hydraulic oils", Rock Valley Oil and Chemical Company, 2007.

Kunal Agarwal. "Analytical and Numerical Investigation of the Heat Dissipation in Couette Flow occurring in the Journal Bearing." IOSR Journal of Mechanical and Civil Engineering (IOSR-JMCE), vol. 16, no. 6, 2019, pp. 28-58